DMT efficiently inhibits hepatic gluconeogenesis by regulating the Gαq signaling pathway

Ting-Ting Zhou[1,2], Fei Ma[3], Xiao-Fan Shi[1,2], Xin Xu[1,2], Te Du[1,2], Xiao-Dan Guo[1,2], Gai-Hong Wang[1], Liang Yu[1,2], Vatcharin Rukachaisirikul[4], Li-Hong Hu[1,2], Jing Chen[1,2] and Xu Shen[1,2,5]

[1]Key Laboratory of Receptor Research, Shanghai Institute of Materia Medica, Chinese Academy of Sciences, Shanghai, China
[2]University of Chinese Academy of Sciences, Beijing, China
[3]School of Pharmacy, East China University of Science and Technology, Shanghai, China
[4]Department of Chemistry, Faculty of Science, Prince of Songkla University, Songkhla, Thailand
[5]Key Laboratory of Drug Target and Drug for Degenerative Disease, School of Medicine and Life Sciences, Nanjing University of Chinese Medicine, Nanjing, China

Correspondence should be addressed to L-H Hu or J Chen or X Shen
Email
lhhu@simm.ac.cn or jingchen@simm.ac.cn or xshen@simm.ac.cn

Journal of Molecular Endocrinology

Abstract

Type 2 diabetes mellitus (T2DM) is a chronic metabolic disease with complicated pathogenesis and targeting gluconeogenesis inhibition is a promising strategy for anti-diabetic drug discovery. G protein-coupled receptors (GPCRs) are classified as distinct families by heterotrimeric G proteins, primarily including Gαs, Gαi and Gαq. Gαs-coupled GPCRs function potently in the regulation of hepatic gluconeogenesis by activating cyclic adenosine monophosphate (cAMP)/protein kinase A (PKA) pathway and Gαi-coupled GPCRs exhibit inhibitory effect on adenylyl cyclase and reduce intracellular cAMP level. However, little is known about the regulation of Gαq-coupled GPCRs in hepatic gluconeogenesis. Here, small-molecule 2-(2,4-dimethoxy-3-methylphenyl)-7-(thiophen-2-yl)-9-(trifluoromethyl)-2,3-dihydropyrido[3′,2′:4,5]thieno[3,2-d]pyrimidin-4(*1H*)-one (DMT) was determined to suppress hepatic glucose production and reduce mRNA levels of gluconeogenic genes. Treatment of DMT in *db/db* mice decreased fasting blood glucose and hemoglobin A1C (HbA1c) levels, while improved glucose tolerance and pyruvate tolerance. Mechanism study demonstrated that DMT-inhibited gluconeogenesis by regulating the Gαq/phospholipase C (PLC)/inositol-1,4,5-triphosphate receptor (IP3R)-mediated calcium (Ca^{2+})/calmodulin (CaM)/phosphatidylinositol-4,5-bisphosphate 3-kinase (PI3K)/protein kinase B (AKT)/forkhead box protein O1 (FOXO1) signaling pathway. To our knowledge, DMT might be the first reported small molecule able to suppress hepatic gluconeogenesis by regulating Gαq signaling, and our current work has also highlighted the potential of DMT in the treatment of T2DM.

Key Words
- Gαq signaling
- hepatic gluconeogenesis
- protein kinase B (AKT)
- type 2 diabetes mellitus (T2DM)

Journal of Molecular Endocrinology
(2017) **59**, 151–169

Introduction

Type 2 diabetes mellitus (T2DM) is a chronic metabolic disease characterized by hyperglycemia, insulin resistance and relative lack of insulin (An & He 2016). T2DM accounts for over 90% of diabetes cases, and its incidence has dramatically increased over the past few decades (Shaw *et al.* 2010, An & He 2016). Although dozens of

http://jme.endocrinology-journals.org
DOI: 10.1530/JME-17-0121

Published by Bioscientifica Ltd.

clinical drugs are currently used for treating T2DM, their varied side effects are commonly determined, such as hypoglycemia, gastrointestinal disturbances, edema, weight gain and lactic acidosis (Moller 2001, Xu *et al.* 2014). For example, glucagon-like peptide-1 receptor agonists (GLP-1 RAs) are newly injectable peptide drugs used for the treatment of hyperglycemia (Scheen 2016). They are known for improving glycemic control with low risk of hypoglycemia, and even reducing cardiovascular disease risk (Dalsgaard *et al.* 2017). However, GLP-1 RAs are associated with gastrointestinal disturbance events, including nausea and vomiting (Peng *et al.* 2016). GLP-1 RAs may also potentially contribute to the development of pancreatitis and increase the risk of pancreatic cancer (Lamont & Andrikopoulos 2014). Thus, it is still urgent to develop new drugs based on new targets or signal(s) against T2DM.

Pathologically, endogenous glucose production from uncontrolled hepatic gluconeogenesis is a major source of fasting hyperglycemia in T2DM patients (An & He 2016), and metformin is being widely used as a first-line oral hypoglycemic drug to treat T2DM. Considering that the hypoglycemic mechanism of metformin is generally believed to be related to its ability in hepatic gluconeogenesis suppression (Inzucchi *et al.* 1998, An & He 2016), appropriate control of hepatic gluconeogenesis is always an attractive strategy for the treatment and prevention of T2DM.

Gluconeogenesis is a metabolic process responsible for glucose generation from certain non-carbohydrate carbon substrates, such as pyruvate, lactate, lipids, glycerol and glucogenic amino acids (Jitrapakdee 2012). In this process, glucose-6-phosphatase (G6Pase) and phosphoenolpyruvate carboxykinase (PEPCK) function as the key rate-limiting regulatory enzymes (Rui 2014). Gluconeogenesis occurs principally in liver and plays an important role in maintaining blood glucose level to avoid hypoglycemia during prolonged starvation (Jitrapakdee 2012). However, patients with T2DM have continuous activated gluconeogenesis and elevated blood glucose level (Yoon *et al.* 2001).

Hepatic gluconeogenesis is highly regulated by hormonal systems in response to fasted and fed states (Jitrapakdee 2012). Insulin suppresses gluconeogenesis through insulin receptor (IR)/IR substrates (IRSs)/phosphatidylinositol-4,5-bisphosphate 3-kinase (PI3K)/protein kinase B (AKT) pathway (Saltiel & Kahn 2001, Rui 2014). Additionally, insulin also suppresses gluconeogenesis by activating salt-inducible kinase 2 (SIK2) leading to cyclic adenosine monophosphate (cAMP) response element-binding protein (CREB)-regulated transcriptional coactivator 2 (CRTC2) phosphorylation and cytoplasmic translocation (Dentin *et al.* 2007). Glucagon binds to glucagon receptor (GCGR), a G protein-coupled receptor (GPCR), and activates Gαs/cAMP/protein kinase A (PKA)/CREB/CRTC2 signaling pathway to stimulate gluconeogenesis (Jiang & Zhang 2003). Activated PKA phosphorylates CREB and promotes CRTC2 dephosphorylation and nuclear transportation (Liu *et al.* 2008) and also activates inositol-1,4,5-triphosphate receptor (IP3R) to increase calcium (Ca^{2+}) release from endoplasmic reticulum (ER) into cytoplasm resulting in the calcineurin-mediated dephosphorylation of CRTC2 (Wang *et al.* 2012).

GPCRs occupy the largest family of receptors in mammalian genome and are classified as distinct families by heterotrimeric G proteins, primarily including Gαs, Gαi and Gαq (Mitchell 2013). GCGR is abundantly expressed in hepatocytes and positively regulates hepatic gluconeogenesis by activating adenylyl cyclase to stimulate cAMP/PKA pathway in a Gαs-dependent manner (Cho *et al.* 2012), while Gαi-coupled GPCRs negatively regulate gluconeogenesis by inactivating adenylyl cyclase (Li *et al.* 2013). However, little is known about the metabolic functions of GPCRs coupled to Gαq protein in liver.

In the current study, we reported that small molecular compound 2-(2,4-dimethoxy-3-methylphenyl)-7-(thiophen-2-yl)-9-(trifluoromethyl)-2,3-dihydropyrido[3′,2′:4,5]thieno[3,2-d]pyrimidin-4(*1H*)-one (DMT, Fig. 1A) antagonized the glucagon-stimulated hepatic gluconeogenesis by regulating the Gαq/phospholipase C (PLC)/IP3R-mediated Ca^{2+}/calmodulin (CaM)/PI3K/AKT/forkhead box protein O1 (FOXO1) signaling pathway. Assay on T2DM model *db/db* mice demonstrated that DMT administration efficiently decreased fasting blood glucose and hemoglobin A1c (HbA1c) levels and improved glucose tolerance and pyruvate tolerance tests. To our knowledge, DMT might be the first reported small molecule as a Gαq signaling regulator with the inhibitory effect on hepatic gluconeogenesis, and the relevant mechanism has been intensively investigated. Moreover, the high efficiency of DMT in improving glucose homeostasis of diabetic mice has highlighted the potential of this agent in the treatment of T2DM.

http://jme.endocrinology-journals.org
DOI: 10.1530/JME-17-0121

Published by Bioscientifica Ltd.

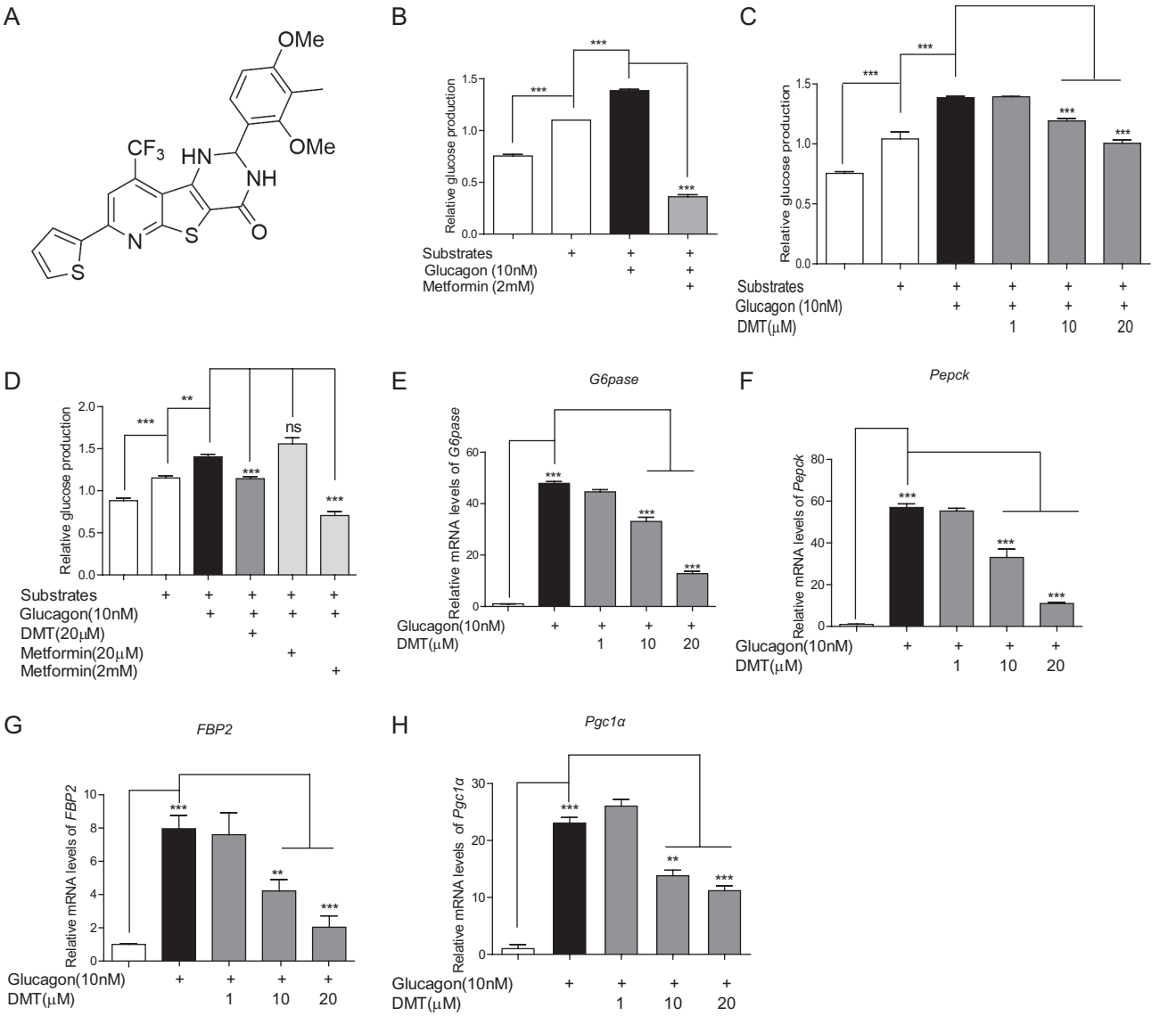

Figure 1

DMT inhibits hepatic gluconeogenesis. (A) Chemical structure of DMT. (B) Primary hepatocytes were treated as indicated, and HGP assay was performed according to the published approach (Zhang *et al*. 2013). Glucagon (10 nM) was used to mimic hyperglucagonemia stimulating excessive gluconeogenesis, and metformin (2 mM) was used as a positive control. (C) DMT (1, 10, 20 μM) inhibited HGP. (D) Metformin (20 μM) did not change the HGP induced by glucagon. (E, F, G and H) Primary hepatocytes were treated with DMT (1, 10, 20 μM) for 24 h, followed by stimulation with glucagon (10 nM) together for another 2 h, and collected for q-PCR assay to determine the mRNA levels of gluconeogenic genes *G6pase*, *Pepck*, *Fbp2* and *Pgc1α*. All data were obtained from three independent experiments and presented as means ± S.E.M. (***P* < 0.01, ****P* < 0.001; ns, no significance).

Materials and methods

Materials and reagents

Glucagon, forskolin (FSK), 2-aminoethoxydiphenyl borate (2-APB), 3-isobutyl-1-methylxanthine (IBMX), pertussis toxin (PTX), collagenase and *N*-(6-aminohexyl)-5-chloro-1-naphthalenesulfonamide hydrochloride (W-7) were purchased from Sigma-Aldrich. U73122 and wortmannin were from Selleck Chemicals (Shanghai, China). Suramin was from J&K Chemical Ltd. (Shanghai, China). DMT was from commercial compound library (SPECS, Holland). Antibodies against phospho-AKT (Ser473), AKT, phospho-IR (Tyr1135/1136), IR, phospho-FOXO1 (Ser256), FOXO1, phospho-CREB (Ser133), CREB, phospho-5′ adenosine monophosphate-activated protein kinase (AMPK) (Thr172), AMPK and Lamin B1 were from Cell Signaling Technology, G6Pase, PEPCK and Gαq was from Santa Cruz Biotechnology and

http://jme.endocrinology-journals.org
DOI: 10.1530/JME-17-0121

Published by Bioscientifica Ltd.

Journal of Molecular Endocrinology

glyceraldehyde-3-phosphate dehydrogenase (GAPDH) was from Kangcheng Bio-tech (Shanghai, China). Gαq-siRNA was purchased from Santa Cruz Biotechnology. Transfection reagent Lipofectamine RNAiMAX was from Invitrogen Company. All media for cell culture, fetal bovine serum (FBS) and antibiotic supplements were from Invitrogen Company. Fluo-4 AM was from Life Technology.

Isolation of mouse primary hepatocytes

Primary hepatocytes were isolated from 9-week-old male C57BL/6 mice fasted overnight with water *ad libitum* by a two-step collagenase perfusion method as previously described with modification (Mathijs *et al*. 2009). Briefly, before isolation, mice were pre-anesthetized and the abdominal cavity and thoracic cavity were opened. The liver was perfused with clear cannulation inserted into the thoracic inferior vena cava and secured with a ligature. The abdominal hepatic inferior vena cava was occluded with forceps and portal vein was cut through allowing outflow of the solution. The liver was perfused with 0.5 mM EGTA-contained phosphate buffered saline (PBS) buffer for about 5 min, and the Dulbecco's modified eagle medium (DMEM) supplemented with collagenase (0.5 mg/mL) was then replaced for 5–10 min. The perfusion velocity was 3 mL/min for the first step and 6 mL/min for the second. The temperature around 37°C was maintained for the entire procedure of perfusion. The swollen liver was rapidly excised from the body cavity and was transferred to an iced sterile petri dish after finishing the perfusion. The gall bladder and needless fascia were removed from the softened liver. The cells were released by disrupting the liver capsule mechanically into iced standard Williams' E medium (containing 10% FBS, 100 U/mL penicillin and 100 mg/mL streptomycin). The cells were isolated from undigested tissue with a sterile 70-μm mesh nylon filter. After centrifugation (700 ***g***/min) at 4°C for 5 min, cells were re-suspended by standard Williams' E medium with 50% Percoll solution and underwent a second centrifugation at 1000 ***g***/min for 10 min to remove dead or low-viability cells. Freshly isolated mouse hepatocytes were seeded at a density of 1.2 million cells per well onto 6-well plates (for quantitative real-time PCR (q-PCR) assay), 0.5 million per well onto 12-well plates (for Western blot assay) or 50,000 per well onto 48-well plates (for hepatic glucose production (HGP) assay) in standard Williams' E medium.

HGP assay

HGP assay was conducted according to the previous study with modification (Zhang *et al*. 2013). In the assay, freshly isolated mouse hepatocytes were seeded onto 48-well plates with standard Williams' E medium. After 4-h attachment, cells were changed to serum-free minimum essential medium (MEM) and incubated with corresponding compounds and 10 nM glucagon for 16 h. After washing with PBS twice to remove the remaining glucose, cells were incubated with compounds and 10 nM glucagon in 200 μL glucose production detection buffer (glucose-free DMEM without phenol red containing 20 mM sodium lactate and 2 mM sodium pyruvate). After 6-h incubation, 50 μL detection buffer was collected for glucose concentration measurement with a colorimetric glucose assay kit (Nanjing Jiancheng, Nanjing, China) according to the manufacturer's instruction. The results were normalized to the total protein concentration measured by BCA protein kit (Thermo Scientific).

RNA isolation and q-PCR assay

Primary hepatocytes were seeded onto 6-well plates. After 4-h attachment, cells were replaced to MEM supplemented with 10% FBS, 100 U/mL penicillin and 100 mg/mL streptomycin. Cells were incubated with corresponding compounds for 24 h and stimulated with 10 nM glucagon together for another 2 h. Total RNA from cultured mouse hepatocytes or mashed liver tissues was extracted using TRIzol reagent according to the manufacturer's protocol (Takara Bio). Complementary DNAs were generated by PrimeScript RT reagent kit (Takara Bio) and analyzed by q-PCR assay using SYBR Premix Ex Taq (Takara Bio) on a Bio-Rad CFX Connect Real-Time System (Bio-Rad Company). The mRNA levels of specific genes were normalized to *Gapdh*. The primers for q-PCR were generated from Sangon Biotech (Shanghai, China) as follows:

G6pase (+), TAATTGGCTCTGCCAATGGCGATC;
G6pase (–), ATCAGTCTGTGCCTTGCCCCTGT;
Pepck (+), CTGCATAACGGTCTGGACTTC;
Pepck(–), CAGCAACTGCCCGTACTCC;
Peroxisome proliferator γ-activated receptor coactivator 1-α (*Pgc1α*) (+), TTCTGGGTGGATTGAAGTGGTC;
Pgc1α (–), TGTCAGTGCATCAATGAGGGC;
Fructose bisphosphatase 2 (*Fbp2*) (+), ACCCGTTACGTTATGGAAAAGG;

http://jme.endocrinology-journals.org
DOI: 10.1530/JME-17-0121

Published by Bioscientifica Ltd.

Fbp2 (–), GGCAGTCAGCATCGAGTTGAG;
Foxo1 (+), AAGTACAGATACGGCCAATCC;
Foxo1 (–), CGTAACTTGATTTGCTGTCCTG;
Gapdh (+), ACAGCAACAGGGTGGTGGAC;
Gapdh (–), TTTGAGGGTGCAGCGAACTT.

Intracellular Ca^{2+} level assay

Intracellular Ca^{2+} level assay was performed as previously described with modification (Yao *et al.* 2015). Primary hepatocytes were seeded onto 96-well plates at a density of 20,000 cells per well and incubated overnight. Cells were loaded with 40 µL of Ca^{2+} dye (Fluo-4 AM, 2 µM) and then incubated at 37°C for 40 min. Intracellular Ca^{2+} level was analyzed by FlexStation II 384 (Molecular Devices, CA, USA) at an excitation wavelength of 490 nm and emission wavelength of 525 nm. After the baseline fluorescence signals were measured for the first 16 s, the corresponding compounds in Hank's balanced salt solution (HBSS) buffer were added to the plate through an automated pipette. Ca^{2+}-free HBSS buffer was used to mimic the extracellular Ca^{2+}-free situation. The relative fluorescence signals were measured at 1.6-s intervals for 80 s, and the data were analyzed and shown as the area under the curve (AUC).

Nuclear and cytosolic protein extraction

Nuclear and cytosolic protein was extracted by the nucleus and cytoplasm extraction kit (Beyotime Institute of Biotechnology, Shanghai, China) according to the manufacturer's instruction. Briefly, primary hepatocytes were incubated with cytosol reagent A supplemented with PMSF on ice for 15 min, and then cytosol reagent B was added, followed by centrifugation to obtain the cytoplasmic protein in the liquid supernatant. The precipitate was re-suspended in nuclear protein extracting solution supplemented with PMSF, followed by vortex and centrifugation to obtain nuclear protein. The contents of nuclear and cytoplasmic protein were measured by BCA protein assay kit (Thermo Scientific).

Western blot assay

Western blot assays were performed as previously described (Zhou *et al.* 2016). Cell or tissue lysate was separated by SDS-PAGE and transferred to the nitrocellulose membrane (GE Health). Membranes were blocked for 1 h in 5% nonfat milk and incubated with corresponding primary antibodies at 4°C overnight. All membranes were subsequently incubated with secondary antibodies for 2 h at room temperature. Membranes were visualized using the West-Dura detection system (Thermo Scientific). The signal was collected by ImageQuant LAS 4000 mini (GE Health).

Intracellular cAMP assay

Primary hepatocytes were seeded onto 96-well plates at a density of 20,000 cells per well and incubated overnight. Cells were treated with corresponding compounds, 3-isobutyl-1-methylxanthine (IBMX) (500 µM) and stimulated with/without FSK (10 µM) or glucagon (10 nM) for 30 min. Intracellular cAMP levels were detected by cAMP-Glo assay kit (Promega).

Whole-cell GCGR-binding assay

Whole-cell GCGR-binding assay was performed as described previously (Siu *et al.* 2013). CHO-K1 cells were seeded onto 96-well poly-D-lysine-treated cell culture plates (PerkinElmer). After overnight culture, the cells were transiently transfected with human GCGR DNA. After 24-h transfection, cells were incubated with blocking buffer (F12 supplemented with 33 mM 4-(2-hydroxyethyl)-1-piperazineethanesulfonic acid (HEPES) and 0.1% bovine serum albumin (BSA), pH 7.4) for 2 h at 37°C, and then incubated with ^{125}I-glucagon (40 pM) and different concentrations of unlabeled glucagon or DMT at room temperature for 3 h. Cells were then washed three times with ice-cold PBS and lysed by 50 µL lysis buffer (PBS supplemented with 20 mM Tris–HCl and 1% Triton X-100, pH 7.4). The radioactivity was counted (counts per minute, CPM) in a scintillation counter (MicroBeta2 Plate Counter, PerkinElmer) using a scintillation cocktail (OptiPhase SuperMix, PerkinElmer).

Animal experiments

All animals were received humane care, and animal-related protocols were approved by the Institutional Animal Care and Use Committees at Shanghai Institute of Materia Medica, Chinese Academy of Sciences. *db/db* male mice (BKS.Cg-*Dock7*$^{m\ +/+}$ *Lepr*^{db}/J) were from Jackson Laboratory. Eight-week-old male mice were housed (n=2–3 per cage) at relative humidity of 50% and a 12-h-light-darkness cycle at 20–22°C, and given *ad libitum*

http://jme.endocrinology-journals.org
DOI: 10.1530/JME-17-0121

Published by Bioscientifica Ltd.

access to water and food. Mice were divided into 2 groups by fasting blood glucose and body weight. Vehicle or DMT (25 mg/kg) was administrated by intraperitoneal injection daily for 5 weeks. Fasting blood glucose levels from 6-h fasted mice were measured weekly, and body weight was recorded twice per week. At the termination of the assay, mice were killed and liver tissues were stored at −80°C for analysis. Alanine aminotransferase (ALT) and aspartate aminotransferase (AST) levels of plasma in *db/db* mice were analyzed with an automatic analyzer (Hitachi 7020, Hitachi).

Oral glucose tolerance test (OGTT) For the glucose tolerance test, the mice were fasted for 16 h at the fourth week, 1.5 g/kg glucose was administered orally with a gavage needle. Glucose levels were measured from tail vein blood samples at 0, 15, 30, 60, 90 and 120 min by ACCU-CHEK active blood sugar system (Roche).

Pyruvate tolerance test (PTT) For the pyruvate tolerance test, the mice were fasted for 16 h at the fifth week and then injected intraperitoneally with sodium pyruvate (1.5 g/kg). Blood glucose levels were measured with tail vein blood samples at 0, 15, 30, 60, 90 and 120 min.

Preliminary pharmacokinetic and tissue distribution assay

18–20 g-weight male C57BL/6 mice ($n=3$) were used for pharmacokinetic study. In the assay, mice were treated with DMT (10 mg/kg) by intraperitoneal injection, and the contents of DMT in plasma were then detected at 0.08, 0.25, 0.5, 1, 2, 4, 8, 24, 48, 72 and 168 h, and data were analyzed with WinNonlin6.4 software to get pharmacokinetic parameters. For tissue distribution assay, 18–20 g-weight male C57BL/6 mice ($n=4$) were treated with DMT (10 mg/kg) by intraperitoneal injection. After 4-h treatment, the mice were killed and blood and organs related to glucose homeostasis, including liver, pancreas and gastrocnemius muscle tissues, were stored to detect the contents of DMT.

Statistical analysis

Significant differences of two groups were compared using Student's *t* test (unpaired, two tailed), and multiple treatment groups were compared within individual experiments by ANOVA test with GraphPad Prism 5 software. All values were presented as mean ± S.E.M. *P* value <0.05 was considered statistically significant. Significant differences were shown as $P<0.05$: *, $P<0.01$: **, $P<0.001$: ***. Unless otherwise indicated, all experiments were repeated at least three times.

Results

DMT inhibits hepatic gluconeogenesis

In the current work, we constructed a screening platform against the lab in-house compound library for assaying the agents able to inhibit HGP from gluconeogenesis with long-time fasting in primary hepatocytes. Given that stimulation of HGP is sustained during long duration of hyperglucagonemia when insulin secretion is inhibited in healthy lean males (Chakravarthy *et al.* 2017), we incubated with glucagon (10 nM) for long time to mimic the pathological state of hyperglucagonemia and stimulate excessive gluconeogenesis in HGP assay. In the assay, sodium lactate (20 mM) and sodium pyruvate (2 mM) were used as gluconeogenic substrates, and compounds (20 μM) were used for screening. The results indicated that metformin (2 mM) as a positive control suppressed HGP (Fig. 1B) and DMT (1, 10, 20 μM) efficiently antagonized the glucagon-stimulated increase in HGP (Fig. 1C). Additionally, metformin (20 μM) could not reduce HGP (Fig. 1D), indicating more potency of DMT than metformin. Moreover, incubation of DMT with glucagon obviously reduced the mRNA levels of gluconeogenic genes *G6pase, Pepck, Fbp2* and *Pgc1α* compared with glucagon treatment results (Fig. 1E, F, G and H). Finally, HGP assay involving glucagon (100 nM) for 5 h was also conducted as previously described (Rah & Kim 2015), and the result (Supplementary Fig. 1A, see section on supplementary data given at the end of this article) indicated that DMT still inhibited the glucagon-induced HGP. Thus, all results demonstrated that DMT inhibits hepatic gluconeogenesis.

DMT represses hepatic gluconeogenesis through Ca^{2+}/CaM/PI3K/AKT/FOXO1 pathway

DMT inhibits gluconeogenesis independently of GCGR In view of the fact that GCGR antagonists function potently in repressing hepatic gluconeogenesis (Rivera *et al.* 2007, Xiong *et al.* 2012) and DMT antagonized the glucagon-stimulated HGP and gluconeogenic genes transcription, we at first investigated whether DMT functioned as a GCGR antagonist. As shown in Fig. 2A,

http://jme.endocrinology-journals.org
DOI: 10.1530/JME-17-0121

Published by Bioscientifica Ltd.

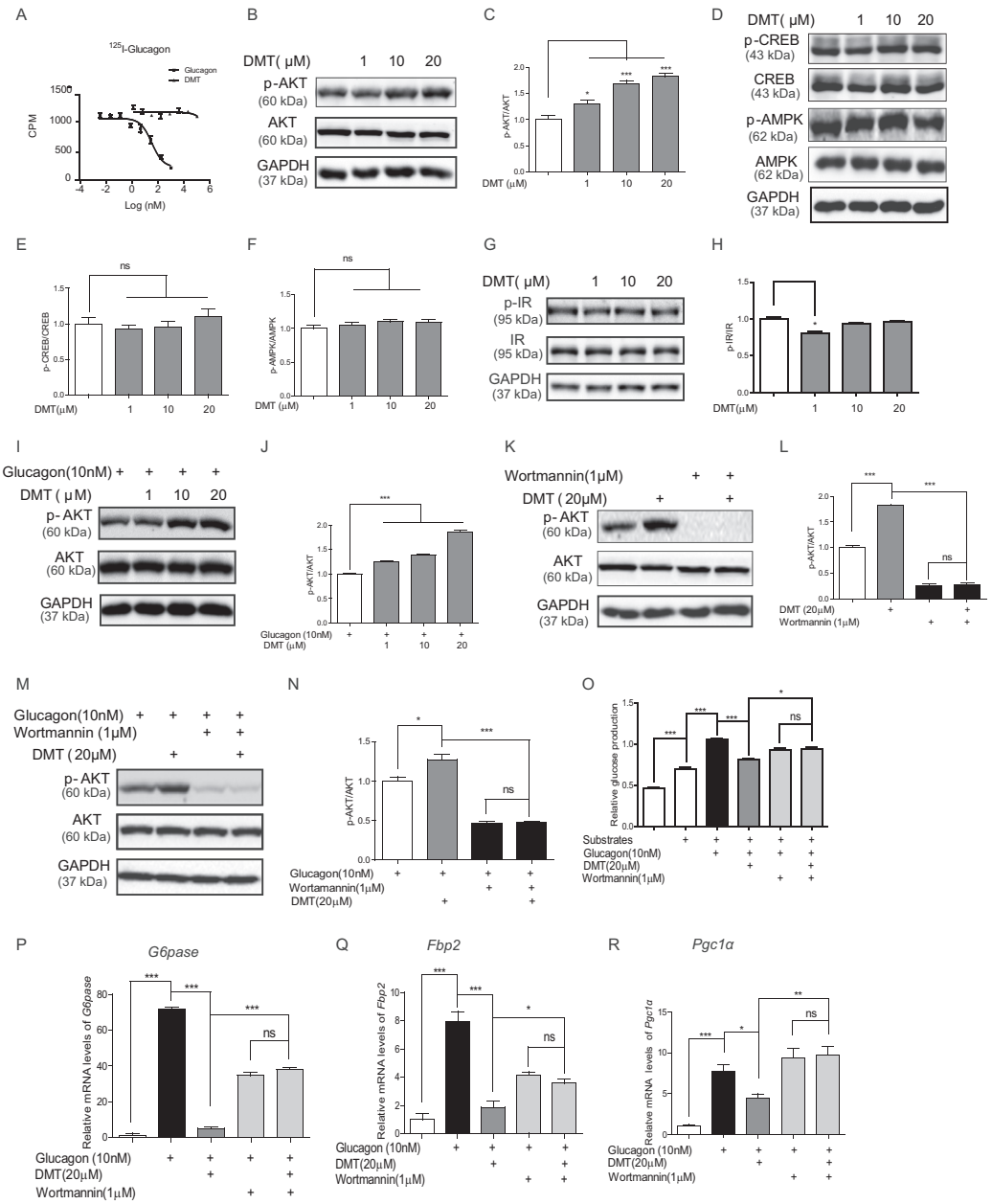

Figure 2

DMT inhibits gluconeogensis through insulin-independent PI3K/AKT pathway. (A) Different concentrations of glucagon or DMT were performed with whole-cell GCGR binding assay. Glucagon was used as a positive control. (B) Primary hepatocytes were treated with DMT (1, 10, 20 μM) for 4 h, and then collected for Western blot assay with antibodies against p-AKT and AKT. (C) Relative levels of p-AKT/AKT in (B) from three independent experiments. (D) Primary hepatocytes were incubated with DMT (1, 10, 20 μM) for 4 h, and then collected for Western blot assay with corresponding antibodies. (E) Relative levels of p-CREB/CREB in (D) from three independent experiments. (F) Relative levels of p-AMPK/AMPK in (D) from three independent experiments. (G) Primary hepatocytes were cultured with DMT (1, 10, 20 μM) for 4 h, and then collected for Western blot assay with antibodies against p-IR and IR. (H) Relative levels of p-IR/IR in (G) from three independent experiments. (I) Primary hepatocytes were cultured with DMT (1, 10, 20 μM) for 3.5 h, followed by co-incubation with glucagon (10 nM) for another 0.5 h, and then collected for Western blot assay with antibodies against p-AKT and AKT. (J) Relative levels of p-AKT/AKT in (I) from three independent experiments. (K) Primary hepatocytes were treated with PI3K inhibitor wortmannin (1 μM) and DMT (20 μM) for 4 h, and then collected for Western blot assay with antibodies against p-AKT and AKT. (L) Relative levels of p-AKT/AKT in (K) from three independent experiments. (M) Primary hepatocytes were pre-incubated with DMT (20 μM) and wortamannin (1 μM) for 3.5 h, followed by stimulation with glucagon (10 nM) for another 0.5 h, and then collected for Western blot assay with antibodies against p-AKT and AKT. (N) Relative levels of p-AKT/AKT in (M) from three independent experiments. (O) HGP assay involving wortmannin (1 μM) was performed as indicated. (P, Q and R) Primary hepatocytes were treated with DMT (20 μM) and wortmannin (1 μM) for 24 h, followed by stimulation with glucagon (10 nM) for another 2 h, and then q-PCR assay was carried out to detect the corresponding mRNA levels of gluconeogenic genes. All data were obtained from three independent experiments and presented as means ± S.E.M. (*$P<0.05$, **$P<0.01$, ***$P<0.001$; ns, no significance).

http://jme.endocrinology-journals.org
DOI: 10.1530/JME-17-0121

Published by Bioscientifica Ltd.

Journal of Molecular Endocrinology

the whole-cell GCGR-binding assay demonstrated that DMT had no affinity against human GCGR (glucagon as a positive control). This result thus indicated that DMT is not a GCGR antagonist and the inhibition of DMT against gluconeogenesis is independent of GCGR.

DMT inhibits gluconeogensis through insulin-independent PI3K/AKT pathway Given that PI3K/AKT and cAMP/PKA pathways are involved in the insulin/glucagon-regulated hepatic gluconeogenesis (Jiang & Zhang 2003, Wang *et al*. 2010) and activated AMPK inhibits hepatic gluconeogenesis by regulating CRTC2 phosphorylation and nuclear translocation (Lee *et al*. 2010), we next investigated the potential of DMT in the regulation of the key proteins involved in these pathways in primary hepatocytes. The results indicated that treatment of DMT for 4 h obviously increased AKT phosphorylation (Fig. 2B and C) but rendered no effects on the phosphorylation of CREB (a downstream protein of cAMP/PKA pathway) or AMPK (Fig. 2D, E and F). Notably, the effect of DMT (20 μM) treated in different times (from 0.5 to 12 h) on AKT phosphorylation (Supplementary Fig. 1B and C) suggested that the incubation time of DMT was set to 4 h. In addition, DMT phosphorylated AKT in the absence of insulin (Fig. 2B and C) and did not phosphorylate IR (Fig. 2G and H), which thereby indicated that DMT activated AKT phosphorylation independently of insulin. Considering that DMT suppressed glucagon-induced hepatic gluconeogenesis, we next detected its potential effect on AKT phosphorylation in the presence of glucagon. As shown in Fig. 2I and J, pre-incubation of DMT for 3.5 h and stimulation with glucagon together for another 0.5 h effectively increased phosphorylated AKT compared with glucagon treatment. However, PI3K inhibitor wortmannin (Walker *et al*. 2000) antagonized the DMT-induced AKT phosphorylation either in the absence (Fig. 2K and L) or presence (Fig. 2M and N) of glucagon and restrained the DMT-inhibited HGP (Fig. 2O). In addition, wortmannin blocked the inhibition of DMT against the glucagon-induced gluconeogenic genes transcription (Fig. 2P, Q and R). Therefore, all results suggested that DMT inhibits gluconeogensis by insulin-independent PI3K/AKT pathway.

FOXO1 is the downstream of DMT-regulated PI3K/AKT pathway FOXO1 as a transcription factor binds directly to the promoters of gluconeogenic genes to increase glucose production (Puigserver *et al*. 2003, Schilling *et al*. 2006) and is inactivated by AKT activation and detained in cytoplasm (Rui 2014). We thus investigated whether FOXO1 was involved in the regulation of DMT. Herein, we found DMT had no effect on mRNA level of FOXO1 (Fig. 3A), but dose dependently stimulated *Foxo1* phosphorylation in the absence or presence of glucagon (Fig. 3B, C, D and E). As shown in Fig. 3F, G and H, the results demonstrated that phosphorylated FOXO1 was detained in cytoplasm. Moreover, wortmannin diminished such effects of DMT on FOXO1 phosphorylation (Fig. 3I, J, K and L). Therefore, these results indicated that FOXO1 is the downstream of DMT-regulated PI3K/AKT pathway.

Ca^{2+}/CaM axis is the upstream of DMT-regulated PI3K/AKT pathway As IR has been found to be not involved in the pathway for DMT-mediated AKT phosphorylation, we next explored the upstream of PI3K/AKT pathway. It is reported that Ca^{2+} as a widespread second messenger controls a variety of cellular processes (Baba & Kurosaki 2016, Dubois *et al*. 2016), and calmodulin (CaM) as a loop-helix-loop Ca^{2+}-binding protein is a downstream transducer of Ca^{2+} responsible for regulating multiple processes in eukaryotic cells (Chin & Means 2000). For example, cytosolic free Ca^{2+} binds to CaM and activates PI3K by direct association with its p85 regulatory subunit resulting in AKT activation (Perez-Garcia *et al*. 2004, Xu *et al*. 2007). With these facts, we thus detected the effect of DMT on intracellular Ca^{2+} level. Interestingly, we found that DMT dose-dependently increased intracellular Ca^{2+} level (Fig. 4A). It is believed that the increase of cytosolic Ca^{2+} was possibly attributed to Ca^{2+} release from Ca^{2+} store rather than Ca^{2+} influx because DMT still increased cytosolic Ca^{2+} in extracellular Ca^{2+}-free situation (Fig. 4B) and such an effect could be abolished by IP3R (a Ca^{2+}-release channel in ER) antagonist 2-aminoethoxydiphenyl borate (2-APB) (Ansari *et al*. 2014) (Fig. 4C).

As shown in Fig. 4D, E, F and G, CaM antagonist W-7 (Bautista-Carbajal *et al*. 2017) blocked the DMT-stimulated increase of AKT phosphorylation in the absence or presence of glucagon, these results thus indicated that the intracellular DMT-mediated Ca^{2+}/CaM axis likely regulated gluconeogenesis through PI3K/AKT pathway. To further verify such regulation, HGP- and q-PCR-related assays were carried out involving W-7. The results demonstrated that W-7 impaired the inhibition of DMT against glucose production (Fig. 4H) and mRNA levels of gluconeogenic genes (Fig. 4I, J and K). These results thereby confirmed that the DMT-induced inhibition against gluconeogenesis involved CaM regulation, further suggesting that

http://jme.endocrinology-journals.org
DOI: 10.1530/JME-17-0121

Published by Bioscientifica Ltd.

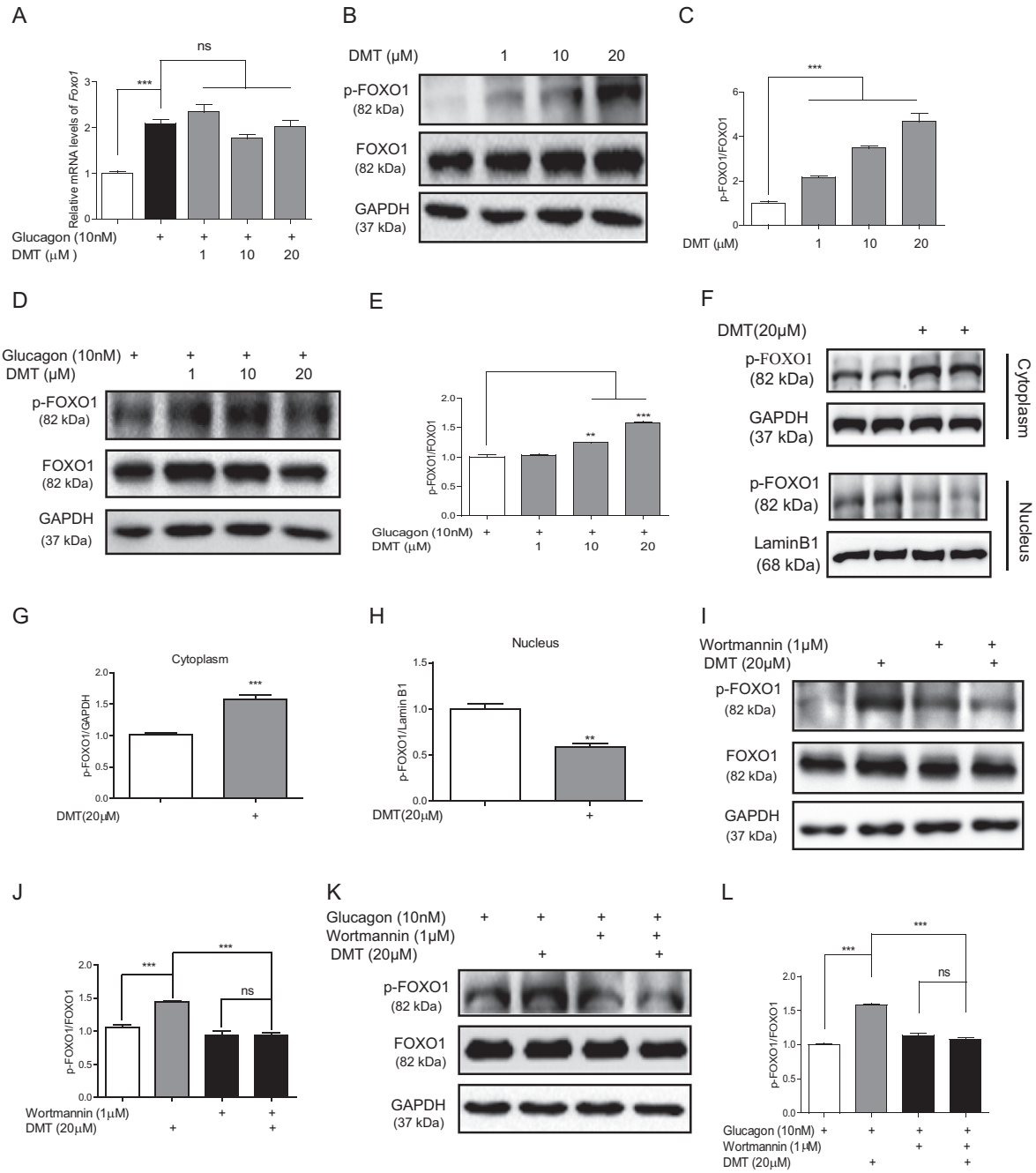

Figure 3

FOXO1 is the downstream of DMT-regulated PI3K/AKT pathway. (A) Primary hepatocytes were cultured with DMT (1, 10, 20 μM) for 24 h, followed by co-incubation with glucagon (10 nM) for another 2 h, and then collected for q-PCR assay to detect the mRNA levels of *Foxo1*. (B) Primary hepatocytes were treated with DMT (1, 10, 20 μM) for 4 h, and then collected for Western blot assay with antibodies against p-FOXO1 and FOXO1. (C) Relative levels of p-FOXO1/FOXO1 in (B) from three independent experiments. (D) Primary hepatocytes were cultured with DMT (1, 10, 20 μM) for 3.5 h, followed by co-incubation with glucagon (10 nM) for another 0.5 h, and then collected for Western blot assay with antibodies against p-FOXO1 and FOXO1. (E) Relative levels of p-FOXO1/FOXO1 in (D) from three independent experiments. (F) Primary hepatocytes were incubated with DMT (20 μM) for 4 h, followed by extraction of nuclear and cytoplasmic protein, and then collected for Western blot assay with antibodies against p-FOXO1. (G and H) Relative levels of p-FOXO1/GAPDH in cytoplasm (G) and p-FOXO1/Lamin B1 in nucleus (H) from three independent experiments. (I) Primary hepatocytes were incubated with DMT (20 μM) and wortamannin (1 μM) for 4 h, and then collected for Western blot assay with antibodies against p-FOXO1 and FOXO1. (J) Relative levels of p-FOXO1/FOXO1 in (I) from three independent experiments. (K) Primary hepatocytes were pre-incubated with DMT (20 μM) and wortamannin (1 μM) for 3.5 h, followed by stimulation with glucagon (10 nM) for another 0.5 h, and then collected for Western blot assay with antibodies against p-FOXO1 and FOXO1. (L) Relative levels of p-FOXO1/FOXO1 in (K) from three independent experiments. All data were obtained from three independent experiments and presented as means ± S.E.M. (**$P<0.01$, ***$P<0.001$; ns, no significance).

http://jme.endocrinology-journals.org
DOI: 10.1530/JME-17-0121

Published by Bioscientifica Ltd.

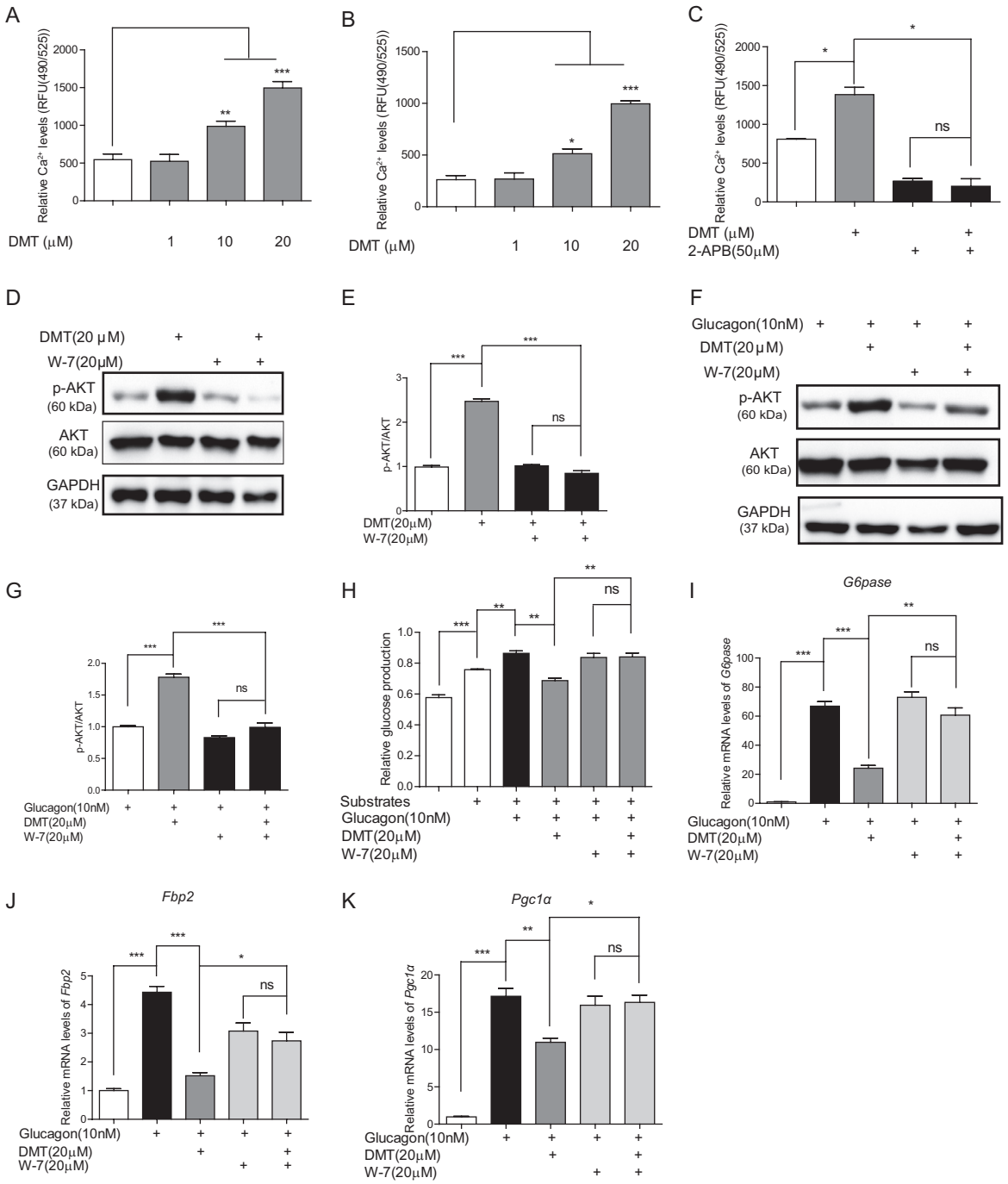

Figure 4

Ca²⁺/CaM axis is the upstream of DMT-regulated PI3K/AKT pathway. (A) Intracellular Ca²⁺ level of primary hepatocytes was detected with FlexStation II 384 according to the previous report (Yao *et al*. 2015). DMT (1, 10, 20 μM) increased intracellular Ca²⁺ level in a dose-dependent manner. (B) DMT (1, 10, 20 μM) increased intracellular Ca²⁺ in extracellular Ca²⁺-free situation. (C) IP3R antagonist 2-APB (50 μM) blocked the increase in DMT-induced intracellular Ca²⁺ level in extracellular Ca²⁺-free situation. (D) Primary hepatocytes were incubated with DMT (20 μM) and CaM antagonist W-7 (20 μM) for 4 h, and then collected for Western blot assay with antibodies against p-AKT and AKT. (E) Relative levels of p-AKT/AKT in (D) from three independent experiments. (F) Primary hepatocytes were pre-incubated with DMT (20 μM) and W-7 (20 μM) for 3.5 h, followed by co-incubation with glucagon (10 nM) for another 0.5 h, and then collected for Western blot assay with antibodies against p-AKT and AKT. (G) Relative levels of p-AKT/AKT in (F) from three independent experiments. (H) HGP assay involving W-7 (20 μM) was performed as indicated. (I, J and K) Primary hepatocytes were treated with DMT (20 μM) and W-7 (20 μM) for 24 h, followed by co-incubation with glucagon (10 nM) for another 2 h, and then collected for q-PCR assay to detect mRNA levels of corresponding gluconeogenic genes. All data were obtained from three independent experiments and presented as means ± S.E.M. (*$P<0.05$, **$P<0.01$, ***$P<0.001$; ns, no significance).

http://jme.endocrinology-journals.org
DOI: 10.1530/JME-17-0121

Published by Bioscientifica Ltd.

Ca^{2+}/CaM axis is the upstream of the DMT-regulated PI3K/AKT pathway.

Taken together, all above-mentioned results fully indicated that DMT represses hepatic gluconeogenesis through Ca^{2+}/CaM/PI3K/AKT/FOXO1 pathway.

DMT inhibits hepatic gluconeogenesis involving Gαq/PLC/IP3R pathway

PLC/IP3R axis is involved in DMT-regulated hepatic gluconeogenesis It has been reported that IP3R as a Ca^{2+}-release channel is necessary for controlling multiple physiological processes through mediating the release of Ca^{2+} from ER (Bosanac *et al*. 2002, Mikoshiba 2015). Phospholipase C (PLC) hydrolyzes phosphatidylinositol 4,5-bisphosphate (PIP2) to produce inositol 1,4,5-trisphosphate (IP3) leading to the activation of IP3R and release of Ca^{2+} from ER (Kohn *et al*. 2015). Given that IP3R antagonist 2-APB alleviated DMT-induced increase in intracellular Ca^{2+} level (Fig. 3C), we next investigated whether PLC/IP3R axis was involved in the mediation of DMT on AKT phosphorylation. As expected,

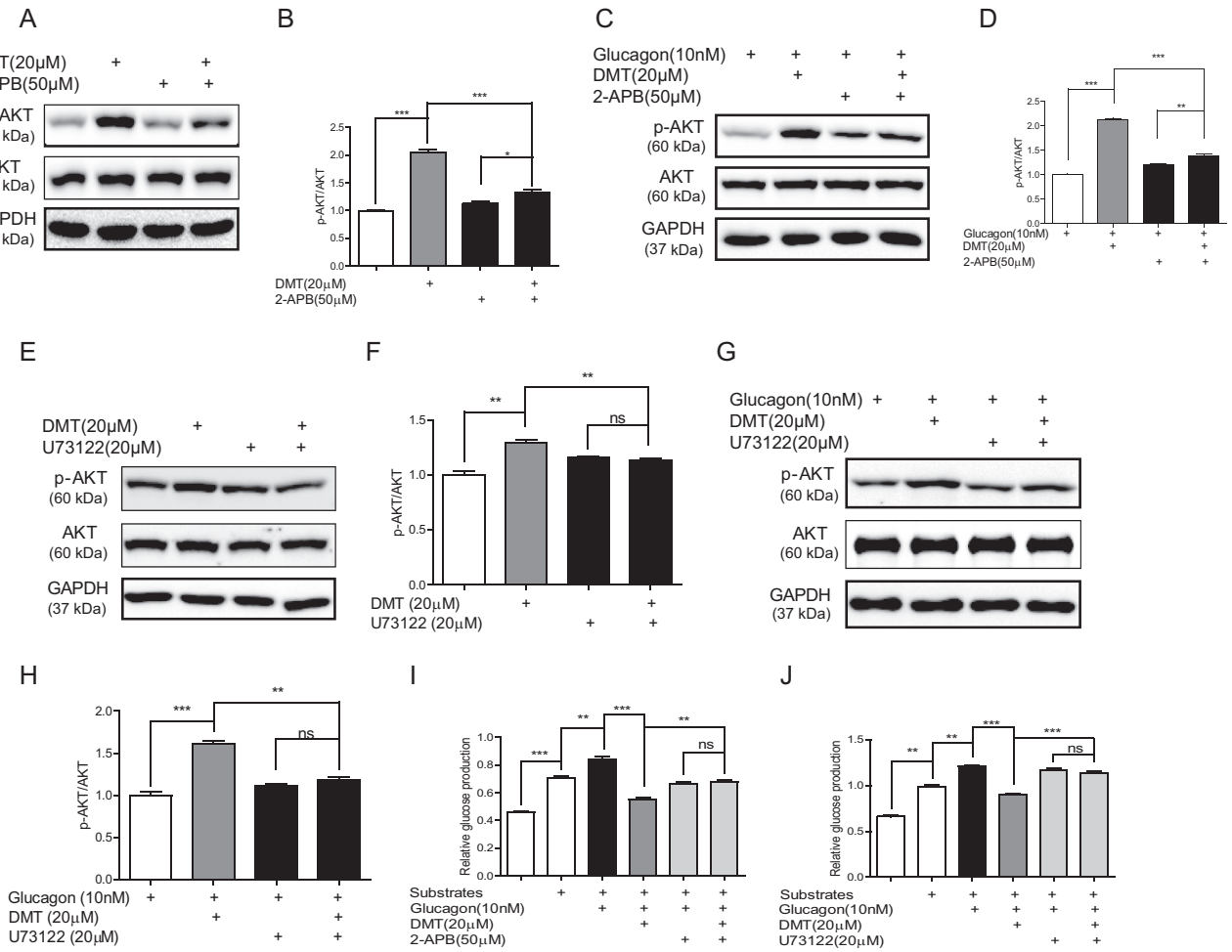

Figure 5

PLC/IP3R axis is involved in DMT-regulated hepatic gluconeogenesis. (A) Primary hepatocytes were incubated with DMT (20 μM) and IP3R antagonist 2-APB (50 μM) for 4 h, and then collected for Western blot assay with antibodies against p-AKT and AKT. (B) Relative levels of p-AKT/AKT in (A) from three independent experiments. (C) Primary hepatocytes were pre-incubated with DMT (20 μM) and 2-APB (50 μM) for 3.5 h, followed by co-incubation with glucagon (10 nM) for another 0.5 h, and then collected for Western blot assay using antibodies against p-AKT and AKT. (D) Relative levels of p-AKT/AKT in (C) from three independent experiments. (E) Primary hepatocytes were incubated with DMT (20 μM) and PLC inhibitor U73122 (20 μM) for 4 h, and then collected for Western blot assay using antibodies against p-AKT and AKT. (F) Relative levels of p-AKT/AKT in (E) from three independent experiments. (G) Primary hepatocytes were pre-incubated with DMT (20 μM) and U73122 (20 μM) for 3.5 h, followed by co-incubation with glucagon (10 nM) for another 0.5 h, and then collected for Western blot assay using antibodies against p-AKT and AKT. (H) Relative levels of p-AKT/AKT in (G) from three independent experiments. (I) HGP assay involving 2-APB (50 μM) was performed as indicated. (J) HGP assay involving U73122 (20 μM) was performed as indicated. All data were obtained from three independent experiments and presented as means ± S.E.M. (*$P<0.05$, **$P<0.01$, ***$P<0.001$; ns, no significance).

http://jme.endocrinology-journals.org
DOI: 10.1530/JME-17-0121

Published by Bioscientifica Ltd.

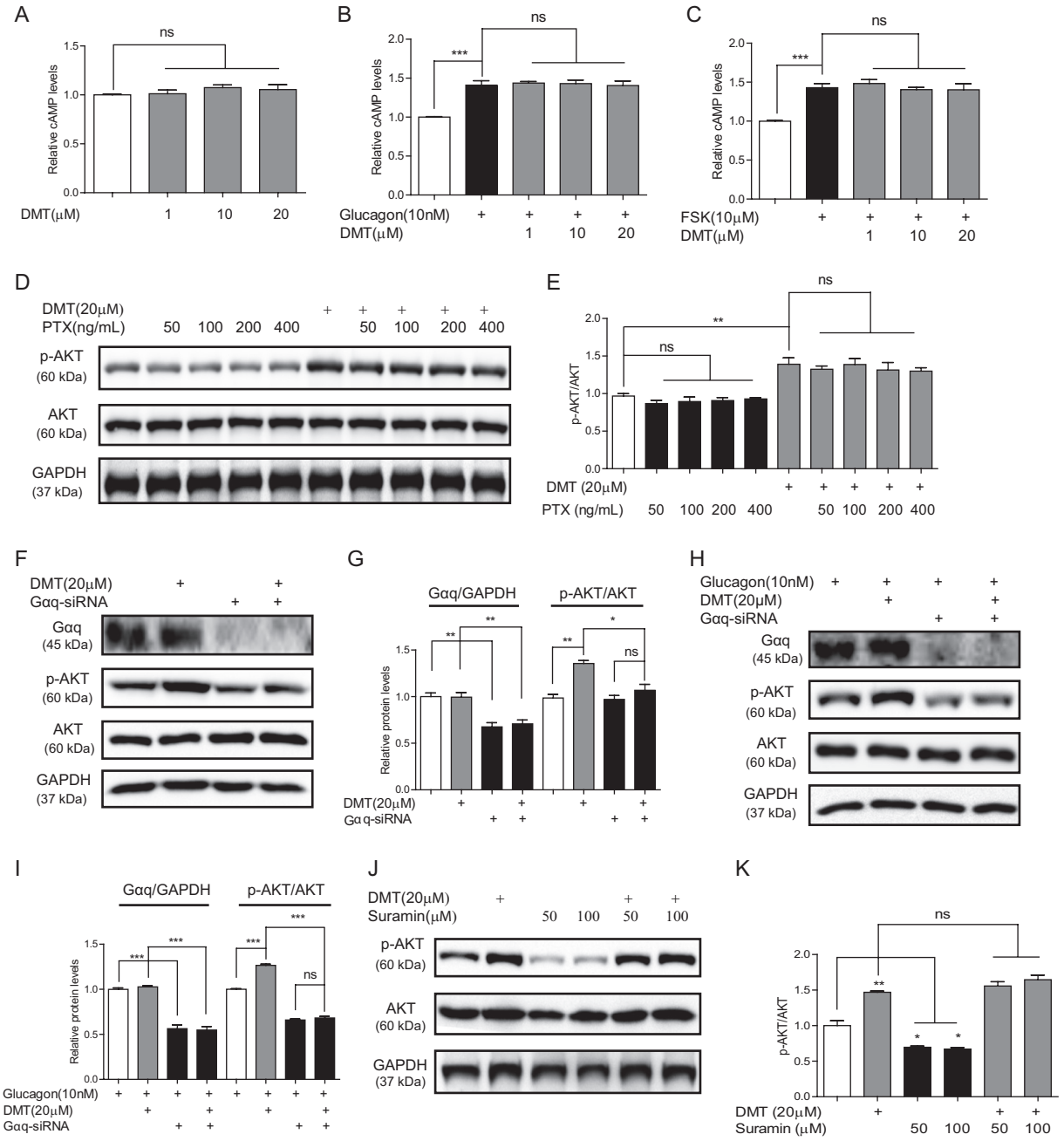

Figure 6

Gαq protein is involved in DMT-regulated AKT phosphorylation. (A) Primary hepatocytes were co-incubated with DMT (1, 10, 20 μM) and IBMX (500 μM) for 0.5 h, and then relative cellular cAMP concentrations were detected following the instructions. (B) Primary hepatocytes were co-incubated with DMT (1, 10, 20 μM), IBMX (500 μM) and glucagon (10 nM) for 0.5 h, and then relative cellular cAMP concentrations were detected following the instructions. (C) Primary hepatocytes were co-incubated with DMT (1, 10, 20 μM), IBMX (500 μM) and FSK (10 μM) for 0.5 h, and then relative cellular cAMP concentrations were detected following the instructions. (D) Primary hepatocytes were pre-incubated with PTX (50, 100, 200, 400 ng/mL) for 2 h, followed by co-incubation with DMT (20 μM) for another 4 h, and then collected for Western blot assay with antibodies against p-AKT and AKT. (E) Relative levels of p-AKT/AKT in (D) from three independent experiments. (F) Primary hepatocytes were transfected with Gαq-siRNA for 48 h, then cultured with DMT (20 μM) for 4 h, and finally collected for Western blot assay with antibodies against p-AKT and AKT. (G) Relative levels of p-AKT/AKT in (F) from three independent experiments. (H) Primary hepatocytes were transfected with Gαq-siRNA for 48 h, then cultured with DMT (20 μM) for 3.5 h, followed by co-incubation with glucagon (10 nM) for 0.5 h, and finally collected for Western blot assay with antibodies against p-AKT and AKT. (I) Relative levels of p-AKT/AKT in (H) from three independent experiments. (J) Primary hepatocytes were pre-incubated with DMT (20 μM) for 3 h, followed by co-incubation with suramin (50, 100 μM) for 1 h, finally collected for Western blot assay with antibodies against p-AKT and AKT. (K) Relative levels of p-AKT/AKT in (J) from three independent experiments. All data were obtained from three independent experiments and presented as means ± S.E.M. (*$P<0.05$, **$P<0.01$, ***$P<0.001$; ns, no significance).

http://jme.endocrinology-journals.org
DOI: 10.1530/JME-17-0121

Published by Bioscientifica Ltd.

Journal of Molecular Endocrinology

either 2-APB (Fig. 5A, B, C and D) or PLC inhibitor U73122 (Leitner *et al*. 2016) (Fig. 5E, F, G and H) repressed the DMT-stimulated AKT phosphorylation in the absence or presence of glucagon. Moreover, either 2-APB (Fig. 5I) or U73122 (Fig. 5J) blocked the inhibition of DMT against HGP. These results thus demonstrated that PLC/IP3R axis is involved in the DMT-regulated hepatic gluconeogenesis.

Gαq protein is involved in DMT-regulated AKT phosphorylation Given that Gαi protein inactivates adenylyl cyclase and reduces intracellular cAMP level (Li *et al*. 2013), and it mediates insulin-regulated AKT phosphorylation to inhibit gluconeogenesis (Yang *et al*. 2013), we wondered whether DMT exhibited capability in regulating Gαi signaling. As indicated in Fig. 6A, B and C, DMT had no effect on intracellular cAMP level in the absence or presence of either glucagon or FSK. These results thereby implied that DMT was not a Gαi signaling regulator. Furthermore, Gαi protein inhibitor pertussis toxin (PTX) (Gao & Jacobson 2016) did not influence the DMT-induced AKT phosphorylation (Fig. 6D and E), further demonstrating that the DMT-increased AKT phosphorylation was independent of Gαi signaling. Considering that Gαq-activated PLC rapidly hydrolyzes PIP2 to increase IP3 and Ca^{2+} levels (Litosch 2016), we next investigated whether Gαq protein participated in the regulation of DMT against AKT phosphorylation. As shown in Fig. 6F, G, H and I, RNA interference mediated by Gαq siRNA remarkably reduced Gαq protein expression and largely resisted DMT-stimulated AKT phosphorylation in hepatocytes transfected with siRNA for 48 h in the absence or presence of glucagon. Therefore, these results demonstrated Gαq protein is involved in DMT-regulated AKT phosphorylation.

It is noted that the first member of family with sequence similarity 3 (FAM3A)-induced AKT phosphorylation could be blocked by Gαq-coupled GPCR P2Y receptor antagonist suramin (Wang *et al*. 2014). However, in our current research, incubation with suramin rendered no influence on the regulation of DMT against AKT phosphorylation (Fig. 6J and K), exhibiting that DMT might directly target Gαq protein or couple to other Gαq-coupled GPCRs except P2Y receptor to regulate Gαq signaling pathway.

Taken together, the above results implied that DMT regulates hepatic gluconeogenesis involving Gαq/PLC/IP3R pathway. It is tentatively suggested that DMT may function as a Gαq signaling regulator to increase intracellular Ca^{2+} level through Gαq/PLC/IP3R pathway and suppress hepatic gluconeogenesis through Ca^{2+}/CaM/PI3K/AKT/FOXO1 pathway.

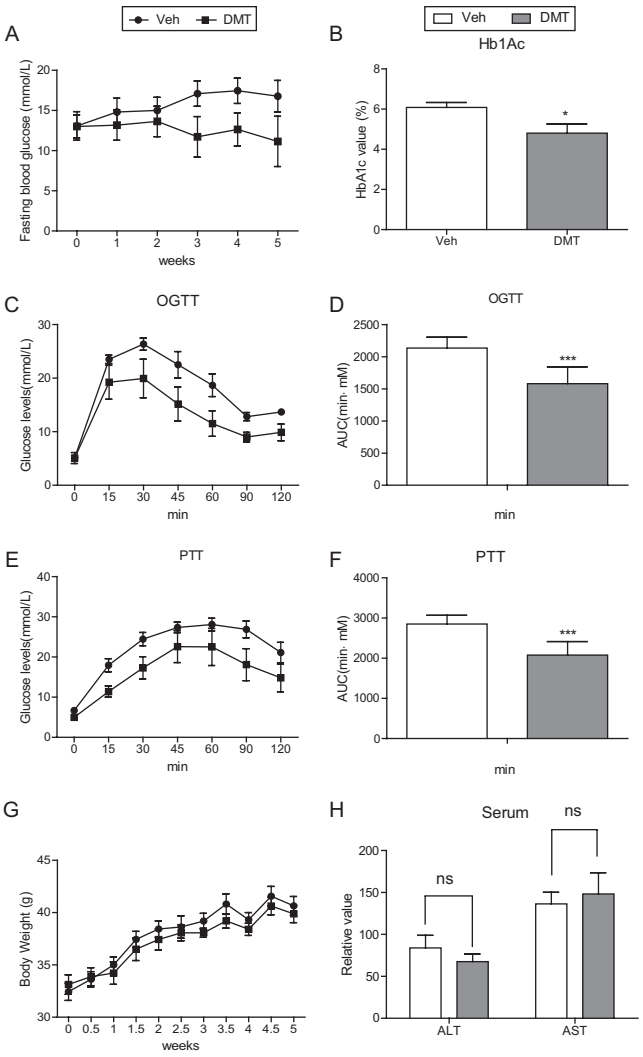

Figure 7
DMT ameliorates hyperglycemia in *db/db* mice. (A) Fasting blood glucose levels were detected weekly in *db/db* mice with treatment of DMT (25 mg/kg/day) ($n=8$). (B) HbA1c levels were determined in *db/db* mice after treatment with DMT for 5 weeks ($n=8$). (C) OGTT assay was performed in *db/db* mice after treatment with DMT (25 mg/kg/day) for 4 weeks ($n=8$). (D) AUC result of OGTT in (C). (E) PTT assay was performed in *db/db* mice after treatment with DMT (25 mg/kg/day) for 5 weeks ($n=8$). (F) AUC result of PTT in (E). (G) The body weight of *db/db* mice with treatment of DMT (25 mg/kg/day) was recorded twice per week ($n=8$). (H) Serum ALT and AST levels were determined in *db/db* mice after treatment with DMT for 5 weeks ($n=8$). All data were presented as means ± S.E.M. (*$P<0.05$, ***$P<0.001$; ns, no significance).

DMT ameliorates hyperglycemia in *db/db* mice

As DMT has been determined to be capable of inhibiting hepatic gluconeogenesis, we next examined its capability in ameliorating hyperglycemia against type 2 diabetic model mice. In the assay, 8-week-old *db/db* male mice were divided into 2 groups and administered with either DMT (25 mg/kg) or vehicle by intraperitoneal

http://jme.endocrinology-journals.org
DOI: 10.1530/JME-17-0121

Published by Bioscientifica Ltd.

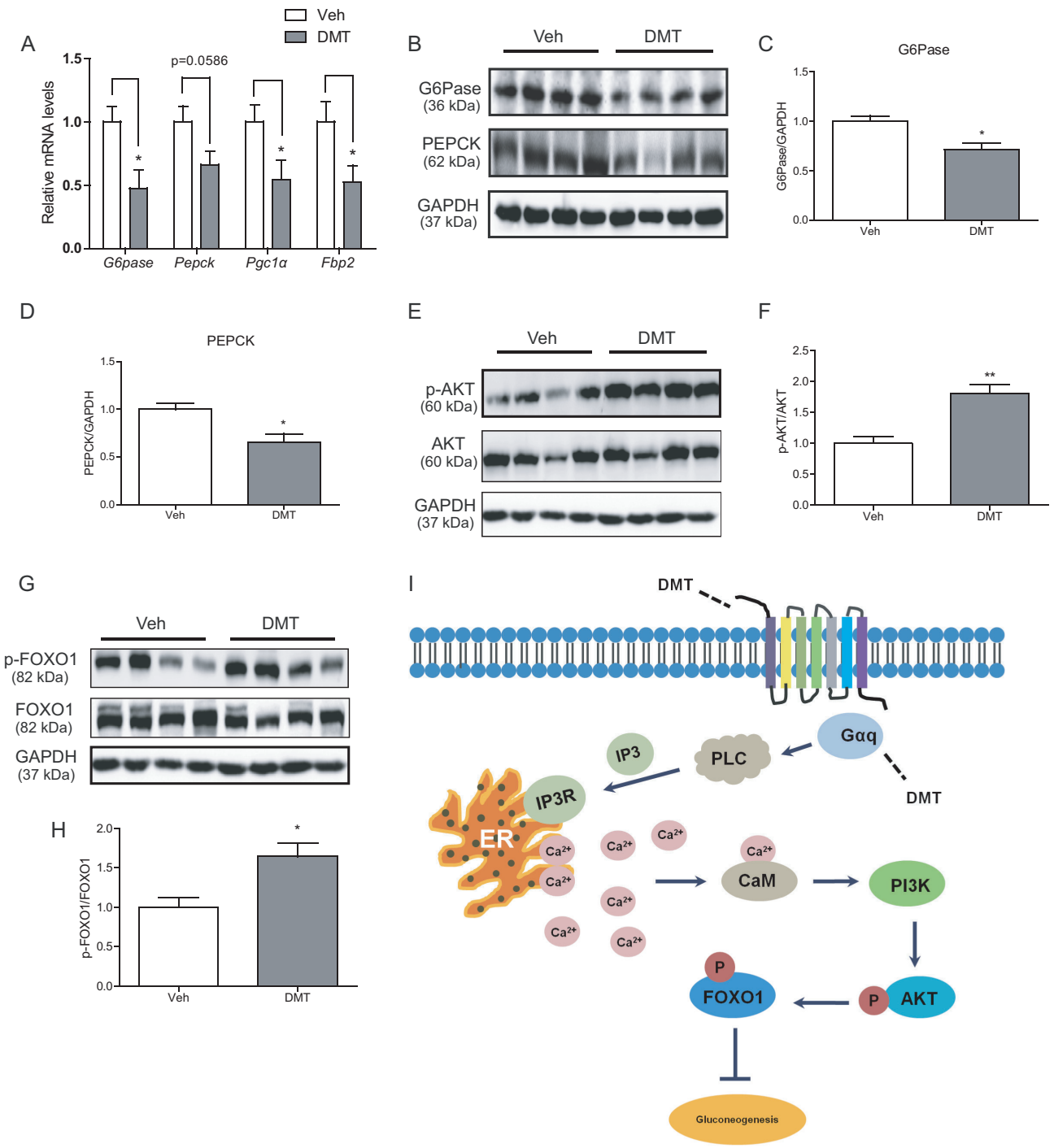

Figure 8

DMT suppresses gluconeogenesis and activates AKT/FOXO1 pathway in *db/db* mice. (A) Liver tissues of *db/db* mice with treatment of DMT (25 mg/kg/day) for 5 weeks were used to perform q-PCR assay to detect the mRNA levels of *G6pase, Pepck, Fbp2* and *Pgc1α* ($n=8$). (B) Liver tissues of *db/db* mice with treatment of DMT (25 mg/kg/day) for 5 weeks were used to perform Western blot assay with corresponding antibodies ($n=4$). (C and D) Relative protein levels of G6Pase/GAPDH (C) and PEPCK/GAPDH (D) in (B). (E) Liver tissues of *db/db* mice with treatment of DMT (25 mg/kg/day) for 5 weeks were used to perform Western blot assay with antibodies against p-AKT and AKT ($n=4$). (F) Relative levels of p-AKT/AKT in (E). (G) Liver tissues of *db/db* mice with treatment of DMT (25 mg/kg/day) for 5 weeks were used to perform Western blot assay with antibodies against p-FOXO1 and FOXO1 ($n=4$). (H) Relative levels of p-FOXO1/FOXO1 in (G). (I) A proposed signaling pathway interpreting the regulation of DMT against hepatic gluconeogensis. DMT activated Gαq signaling to increase intracellular Ca^{2+} level through Gαq/PLC/IP3R pathway. The increased Ca^{2+} bound to CaM and regulated the PI3K/AKT pathway to stimulate phosphorylation of transcription factor FOXO1 and suppress gluconeogenesis through inhibiting gluconeogenic genes transcription. All data were presented as means ± S.E.M. (*$P<0.05$, **$P<0.01$).

http://jme.endocrinology-journals.org
DOI: 10.1530/JME-17-0121

Published by Bioscientifica Ltd.

Journal of Molecular Endocrinology

injection for 5 weeks. The results demonstrated that DMT treatment reduced the fasting blood glucose (Fig. 7A) and HbA1c (Fig. 7B) levels and improved the glucose tolerance (Fig. 7C and D) and pyruvate tolerance (Fig. 7E and F). Additionally, the results in Fig. 7G and H showed that DMT administration did not obviously change body weight, alanine aminotransferase (ALT) or aspartate aminotransferase (AST) levels of plasma in *db/db* mice, suggesting that administration of DMT (25 mg/kg/day) for 5 weeks exerted no apparently hepatic toxicity of *db/db* mice. All the results thus indicated that DMT ameliorates hyperglycemia in *db/db* mice.

DMT suppresses hepatic gluconeogenesis and activates AKT/FOXO1 pathway in *db/db* mice

Given that DMT could inhibit gluconeogensis in hepatocytes and improve pyruvate tolerance *in vivo*, we next evaluated its activity in suppressing gluconeogenesis in the liver tissues of *db/db* mice. As shown in Fig. 8A, B, C and D, DMT administration inhibited mRNA levels of *G6pase, Pepck, Fbp2* and *Pgc1α* and reduced protein expressions of G6Pase and PEPCK. In view of the cell-based result that AKT/FOXO1 pathway was involved in DMT-mediated hepatic gluconeogenesis, we also evaluated the regulation of DMT against this pathway *in vivo*. The results demonstrated that DMT treatment increased the phosphorylation levels of AKT and FOXO1 (Fig. 8E, F, G and H), which was consistent with the cell-based results (Figs 2B and 3B). All results suggested that DMT suppresses hepatic gluconeogenesis and activates AKT/FOXO1 pathway in *db/db* mice.

Discussion

T2DM is a chronic metabolic disease bringing heavy burdens to societies (Zimmet *et al*. 2001). Although the underlying pathological basis of T2DM is obscure, continuous activated gluconeogenesis increases HGP and elevates blood glucose level in T2DM (Yoon *et al*. 2001, Inzucchi *et al*. 2012), and reducing HGP is believed to be an ideal strategy for reducing blood glucose (Zheng *et al*. 2015). It has been found that metformin efficiently improves hyperglycemia primarily through suppressing gluconeogenesis (Rena *et al*. 2013), but lactic acidosis is one of its side effects, which has limited the application of metformin (Li *et al*. 2016, Omar *et al*. 2016). Here, we found that DMT was effective in suppressing HGP and inhibiting gluconeogenic genes transcription and *in vivo* assay results demonstrated that DMT could improve glucose homeostasis. The reduction of gluconeogenesis evoked by metformin may be a result of an inhibition of mitochondrial respiratory chain complex I, AMP deaminase and mitochondrial glycerophosphate dehydrogenase (An & He 2016). However, DMT-inhibited gluconeogenesis involves PI3K/AKT/FOXO1 signaling pathway regulated by Gαq/PLC/IP3R/Ca^{2+} axis, and DMT did not increase the lactate production in hepatocytes and serum (Supplementary Fig. 1E and F). All results have highlighted the potency of targeting gluconeogenesis inhibition in the treatment of T2DM and the potential of DMT as an anti-T2DM drug lead compound. The small molecule DMT was determined by cell-based screening against the lab in-house compound library partly purchased from SPECS commercial company. To date, there is no report on the bioactivity of DMT, although DMT shares the similar structural skeleton to that of thienopyridine, whose derivatives exhibit anti-bacterial, anti-fungal and anti-tumoral activities (Hayakawa *et al*. 2004, Khidre *et al*. 2011). Our current work has thus firstly expanded the pharmacological applications of this kind of compounds in suppressing hepatic gluconeogenesis and potentially treating T2DM.

It is well known that intracellular free Ca^{2+} comes from extracellular Ca^{2+} influx and/or the release from Ca^{2+} storages. Mitochondria and ER are the storehouses of Ca^{2+} in charge of accumulating and releasing Ca^{2+} under certain cellular events (Pinto *et al*. 2015). Activated Gαq protein causes PLC activation leading to the generation of IP3 and the release of Ca^{2+} from ER (Hubbard & Hepler 2006, Li *et al*. 2013). Gαq protein is necessary for the insulin-induced translocation of glucose transporter 4 (GLUT4) in 3T3-L1 adipocytes (Sanchez-Fernandez *et al*. 2014). Unfortunately, the metabolic roles of hepatic Gαq-coupled GPCRs are less well defined *in vivo*. Reports demonstrated that hepatocytes express several Gαq-coupled GPCRs that are also expressed in many other tissues (Regard *et al*. 2008). It is reported that selectively stimulating Gαq-linked GPCR in hepatocytes may increase blood glucose level and impair glucose tolerance (Li *et al*. 2013). Activation of P2Y receptor inhibits hepatic gluconeogenesis and lipogenesis involving PI3K/AKT signaling pathway in a CaM-dependent manner (Wang *et al*. 2014). Gluconeogenesis and glycogenolysis increase in the mice with deficiency of the ghrelin, an endogenous ligand of ghrelin receptor belonging to a Gαq-coupled GPCR (Chacko *et al*. 2012, Damian *et al*. 2015).

http://jme.endocrinology-journals.org
DOI: 10.1530/JME-17-0121

Published by Bioscientifica Ltd.

Table 1 Plasma concentrations (ng/mL) and pharmacokinetic parameters of DMT in C57BL/6 mice treated with DMT (10 mg/kg) by intraperitoneal injection.

	Concentrations (ng/mL) of DMT in plasma ($n=3$)				
Time (h)	Mouse-1	Mouse-2	Mouse-3	Mean	S.D.
0.08	3384.2	3185.6	3233.3	3267.7	103.7
0.25	8493.4	9872.4	7908.3	8758.0	1008.4
0.5	15,709.3	14,885.1	12,532.6	14,375.7	1648.5
1	18,329.7	20,930.8	16,829.4	18,696.6	2075.2
2	21,660.3	25,529.5	20,435.7	22,541.8	2658.9
4	22,872.7	26,921.8	19,348.8	23,047.8	3789.5
8	18,588.2	24,892.2	19,231.8	20,904.1	3468.8
24	17,081.6	15,923.2	15,310.7	16,105.2	899.4
48	13,902.1	15,142.7	14,363.4	14,469.4	627.1
72	9809.7	13,361.0	13,149.4	12,106.7	1992.1
168	7707.1	7235.4	7269.0	7403.8	263.2
HL_Lambda_z ($T_{1/2}$, h)	124.11	111.41	129.01	121.51	9.08
T_{max}(h)	4.00	4.00	2.00	3.33	1.15
C_{max} (ng/mL)	22,872.7	26,921.8	20,435.7	23,410.07	3276.27
AUC_{last} (h*ng/mL)	1,939,043.7	2,218,655.3	2,086,094.6	2,081,264.56	139,868.37
AUC_{INF_pred} (h*ng/mL)	3,213,734.2	3,384,747.7	3,467,947.9	3,355,476.61	129,609.97
MRT_{last} (h)	67.34	64.71	67.67	66.57	1.62
Vz_F_{pred} (L/kg)	0.56	0.47	0.54	0.52	0.04
Cl_F_{pred} (L/h/kg)	0.0031	0.0030	0.0029	0.0030	0.0001
λz calculation time range (h)	8–168	48–168	24–168	NA	NA

We herein found that DMT, as a Gαq signaling regulator, suppressed hepatic gluconeogenesis through Gαq/PLC/IP3R-mediated Ca^{2+}/CaM/PI3K/AKT/FOXO1 pathway. In the previous work, the Gαq-linked designer receptor overexpressed in transgenic mouse was a mutant M_3 muscarinic receptor, and V1b vasopressin receptor expression was enhanced in *ob/ob* mice (Li *et al*. 2013). To our knowledge, M_3 muscarinic receptor and V1b vasopressin receptor belong to Gαq-coupled GPCRs, but they are not representative of all Gαq-coupled GPCRs or endogenous Gαq signaling (Li *et al*. 2009). In our current study, we used RNA interference technology to knockdown endogenous Gαq protein finding that the regulation of DMT against AKT phosphorylation was dependent on Gαq protein. Our results tentatively suppose that activation of Gαq signaling probably suppresses hepatic gluconeogenesis in line with another published report (Wang *et al*. 2014).

It has been reported that effects of Gαq on AKT varies depending on cell types. For example, activated Gαq inhibited PI3K/AKT pathway independently of PLC in 293 cells (Ballou *et al*. 2003), and Gαq-coupled receptors such as bradykinin, thrombin and carbachol increase AKT phosphorylation in different cells (Sanchez-Fernandez *et al*. 2014). Additionally, Gαq inhibitor UBO-QIC inhibits AKT signaling stimulated by P2Y receptor (Gao & Jacobson 2016). In our current research, RNA interference of Gαq apparently abolished the DMT-stimulated AKT phosphorylation, and further investigation suggested that Gαq/PLC/IP3R signaling might be involved in the DMT-inhibited hepatic gluconeogenesis through Ca^{2+}/CaM/PI3K/AKT/FOXO1 pathway, while P2Y receptor was not involved in the regulation of DMT. Although the specific Gαq-coupled GPCR involved in DMT regulation or whether DMT directly activates Gαq is still needed to be further investigated, DMT as a small-molecule

Table 2 Plasma concentrations (ng/mL) and liver/pancreas/gastrocnemius muscle concentrations (ng/g) of DMT in C57BL/6 mice treated with DMT (10 mg/kg) for 4 h by intraperitoneal injection.

Time (h)	**Mice** ($n=4$)	**Plasma** (ng/mL)	**Liver** (ng/g)	**Pancreas** (ng/g)	**Muscle** (ng/g)
4	Mouse-1	47,949.8	16,482.4	8893.5	1543.3
	Mouse-2	47,486.1	12,393.7	6043.4	1289.2
	Mouse-3	40,777.3	12,665.4	6801.3	1312.3
	Mouse-4	43,640.9	16,825.6	7500.9	1411.3
	Mean	44,963.5	14,591.8	7309.8	1389.0
	S.D.	3393.9	2387.9	1212.0	115.7

http://jme.endocrinology-journals.org
DOI: 10.1530/JME-17-0121

Published by Bioscientifica Ltd.

probe may help better understand Gαq signaling and hepatic gluconeogenesis. Since GPCRs are determined to be targets of various pharmaceutical drugs and G proteins can be regulated by GPCRs, small molecules that directly modulate G proteins have become promising therapeutic agents (Nishimura *et al*. 2010). In addition, structural biology might help illustrate the underlying modulatory basis between small molecules and targeted GPCRs or G proteins and highlight the potential of the agents in drug design (Nishimura *et al*. 2010). Preliminary pharmacokinetic study implied that DMT exerted a quick absorption and a slow elimination in mice by intraperitoneal injection, and the maximum plasma concentration turned up around 4 h with a half-life around 120 h (Table 1 and Supplementary Fig. 1D). Tissue distribution assay indicated that DMT was distributed in several main organs related to glucose homeostasis, including liver, pancreas and gastrocnemius muscle (Table 2). It is noted that the table did not involve DMT content in adipose tissue, because of some difficulties in extracting the adipose tissue from abdominal cavity in the assay, although DMT content investigation in adipose tissue should be further supplemented in DMT-based drug discovery.

In conclusion, we have identified that small-molecule DMT suppressed hepatic gluconeogenesis involving Gαq/PLC/IP3R-mediated Ca^{2+}/CaM/PI3K/AKT/FOXO1 pathway. To our knowledge, DMT might be the first reported small molecule as a Gαq signaling regulator functioning in hepatic gluconeogenesis inhibition. Our findings have also highlighted the potential of DMT in the treatment of T2DM.

Supplementary data

This is linked to the online version of the paper at http://dx.doi.org/10.1530/JME-17-0121.

Declaration of interest

The authors declare that there is no conflict of interest that could be perceived as prejudicing the impartiality of the research reported.

Funding

This work was supported by the National Natural Science Foundation of China (grant number 81473141), NSFC-TRF collaboration projects (grant numbers NSFC81561148011 and DBG5980001), Key Laboratory of Receptor Research of the Chinese Academy of Sciences (grant number SIMM1606YZZ-04), Personalized Medicines: Molecular Signature-based Drug Discovery and Development, Strategic Priority Research Program of the Chinese Academy of Sciences (grant number XDA12040313) and the Priority Academic Program Development of Jiangsu Higher Education Institutions (Integration of Chinese and Western Medicine).

References

An H & He L 2016 Current understanding of metformin effect on the control of hyperglycemia in diabetes. *Journal of Endocrinology* **228** R97–R106. (doi:10.1530/JOE-15-0447)

Ansari N, Hadi-Alijanvand H, Sabbaghian M, Kiaei M & Khodagholi F 2014 Interaction of 2-APB, dantrolene, and TDMT with IP3R and RyR modulates ER stress-induced programmed cell death I and II in neuron-like PC12 cells: an experimental and computational investigation. *Journal of Biomolecular Structure and Dynamics* **32** 1211–1230. (doi:10.1080/07391102.2013.812520)

Baba Y & Kurosaki T 2016 Role of calcium signaling in B cell activation and biology. *Current Topics in Microbiology and Immunology* **393** 143–174. (doi:10.1007/82_2015_477)

Ballou LM, Lin HY, Fan GF, Jiang YP & Lin RZ 2003 Activated G alpha q inhibits p110 alpha phosphatidylinositol 3-kinase and Akt. *Journal of Biological Chemistry* **278** 23472–23479. (doi:10.1074/jbc.M212232200)

Bautista-Carbajal P, Soto-Acosta R, Angel-Ambrocio AH, Cervantes-Salazar M, Loranca-Vega CI, Herrera-Martinez M & del Angel RM 2017 The calmodulin antagonist W-7 (N-(6-aminohexyl)-5-chloro-1-naphthalenesulfonamide hydrochloride) inhibits DENV infection in Huh-7 cells. *Virology* **501** 188–198. (doi:10.1016/j.virol.2016.12.004)

Bosanac I, Alattia JR, Mal TK, Chan J, Talarico S, Tong FK, Tong KI, Yoshikawa F, Furuichi T, Iwai M, *et al*. 2002 Structure of the inositol 1,4,5-trisphosphate receptor binding core in complex with its ligand. *Nature* **420** 696–700. (doi:10.1038/nature01268)

Chacko SK, Haymond MW, Sun Y, Marini JC, Sauer PJ, Ma X & Sunehag AL 2012 Effect of ghrelin on glucose regulation in mice. *American Journal of Physiology: Endocrinology and Metabolism* **302** E1055–E1062. (doi:10.1152/ajpendo.00445.2011)

Chakravarthy M, Parsons S, Lassman ME, Butterfield K, Lee AYH, Chen Y, Previs S, Spond J, Yang S, Bock C, *et al*. 2017 Effects of 13-hour hyperglucagonemia on energy expenditure and hepatic glucose production in humans. *Diabetes* **66** 36–44. (doi:10.2337/db16-0746)

Chin D & Means AR 2000 Calmodulin: a prototypical calcium sensor. *Trends in Cell Biology* **10** 322–328. (doi:10.1016/S0962-8924(00)01800-6)

Cho YM, Merchant CE & Kieffer TJ 2012 Targeting the glucagon receptor family for diabetes and obesity therapy. *Pharmacology and Therapeutics* **135** 247–278. (doi:10.1016/j.pharmthera.2012.05.009)

Dalsgaard NB, Bronden A, Vilsboll T & Knop FK 2017 Cardiovascular safety and benefits of GLP-1 receptor agonists. *Expert Opinion on Drug Safety* **16** 351–363. (doi:10.1080/14740338.2017.1281246)

Damian M, Mary S, Maingot M, M'Kadmi C, Gagne D, Leyris JP, Denoyelle S, Gaibelet G, Gavara L, Garcia-de-Souza-Costa M, *et al*. 2015 Ghrelin receptor conformational dynamics regulate the transition from a preassembled to an active receptor:Gq complex. *PNAS* **112** 1601–1606. (doi:10.1073/pnas.1414618112)

Dentin R, Liu Y, Koo SH, Hedrick S, Vargas T, Heredia J, Yates J 3rd & Montminy M 2007 Insulin modulates gluconeogenesis by inhibition of the coactivator TORC2. *Nature* **449** 366–369. (doi:10.1038/nature06128)

Dubois C, Prevarskaya N & Vanden Abeele F 2016 The calcium-signaling toolkit: updates needed. *Biochimica et Biophysica Acta* **1863** 1337–1343. (doi:10.1016/j.bbamcr.2015.11.033)

Gao ZG & Jacobson KA 2016 On the selectivity of the Galphaq inhibitor UBO-QIC: a comparison with the Galphai inhibitor pertussis toxin. *Biochemical Pharmacology* **107** 59–66. (doi:10.1016/j.bcp.2016.03.003)

Hayakawa I, Shioya R, Agatsuma T, Furukawa H & Sugano Y 2004 Thienopyridine and benzofuran derivatives as potent anti-tumor

Published by Bioscientifica Ltd.

agents possessing different structure-activity relationships. *Bioorganic and Medicinal Chemistry Letters* **14** 3411–3414. (doi:10.1016/j.bmcl.2004.04.079)

Hubbard KB & Hepler JR 2006 Cell signalling diversity of the Gqalpha family of heterotrimeric G proteins. *Cell Signaling* **18** 135–150. (doi:10.1016/j.cellsig.2005.08.004)

Inzucchi SE, Maggs DG, Spollett GR, Page SL, Rife FS, Walton V & Shulman GI 1998 Efficacy and metabolic effects of metformin and troglitazone in type II diabetes mellitus. *New England Journal of Medicine* **338** 867–872. (doi:10.1056/NEJM199803263381303)

Inzucchi SE, Bergenstal RM, Buse JB, Diamant M, Ferrannini E, Nauck M, Peters AL, Tsapas A, Wender R, Matthews DR, *et al*. 2012 Management of hyperglycemia in type 2 diabetes: a patient-centered approach: position statement of the American Diabetes Association (ADA) and the European Association for the Study of Diabetes (EASD). *Diabetes Care* **35** 1364–1379. (doi:10.2337/dc12-0413)

Jiang G & Zhang BB 2003 Glucagon and regulation of glucose metabolism. *American Journal of Physiology: Endocrinology and Metabolism* **284** E671–E678. (doi:10.1152/ajpendo.00492.2002)

Jitrapakdee S 2012 Transcription factors and coactivators controlling nutrient and hormonal regulation of hepatic gluconeogenesis. *International Journal of Biochemistry and Cell Biology* **44** 33–45. (doi:10.1016/j.biocel.2011.10.001)

Khidre RE, Abu-Hashem AA & El-Shazly M 2011 Synthesis and antimicrobial activity of some 1-substituted amino-4,6-dimethyl-2-oxo-pyridine-3-carbonitrile derivatives. *European Journal of Medicinal Chemistry* **46** 5057–5064. (doi:10.1016/j.ejmech.2011.08.018)

Kohn E, Katz B, Yasin B, Peters M, Rhodes E, Zaguri R, Weiss S & Minke B 2015 Functional cooperation between the IP3 receptor and phospholipase C secures the high sensitivity to light of Drosophila photoreceptors in vivo. *Journal of Neuroscience* **35** 2530–2546. (doi:10.1523/JNEUROSCI.3933-14.2015)

Lamont BJ & Andrikopoulos S 2014 Hope and fear for new classes of type 2 diabetes drugs: is there preclinical evidence that incretin-based therapies alter pancreatic morphology? *Journal of Endocrinology* **221** T43–T61. (doi:10.1530/JOE-13-0577)

Lee JM, Seo WY, Song KH, Chanda D, Kim YD, Kim DK, Lee MW, Ryu D, Kim YH, Noh JR, *et al*. 2010 AMPK-dependent repression of hepatic gluconeogenesis via disruption of CREB.CRTC2 complex by orphan nuclear receptor small heterodimer partner. *Journal of Biological Chemistry* **285** 32182–32191. (doi:10.1074/jbc.M110.134890)

Leitner MG, Michel N, Behrendt M, Dierich M, Dembla S, Wilke BU, Konrad M, Lindner M, Oberwinkler J & Oliver D 2016 Direct modulation of TRPM4 and TRPM3 channels by the phospholipase C inhibitor U73122. *British Journal of Pharmacology* **173** 2555–2569. (doi:10.1111/bph.13538)

Li JH, Gautam D, Han SJ, Guettier JM, Cui YH, Lu HY, Deng CX, O'Hare J, Jou W, Gavrilova O, *et al*. 2009 Hepatic muscarinic acetylcholine receptors are not critically involved in maintaining glucose homeostasis in mice. *Diabetes* **58** 2776–2787. (doi:10.2337/db09-0522)

Li JH, Jain S, McMillin SM, Cui Y, Gautam D, Sakamoto W, Lu H, Jou W, McGuinness OP, Gavrilova O, *et al*. 2013 A novel experimental strategy to assess the metabolic effects of selective activation of a G(q)-coupled receptor in hepatocytes in vivo. *Endocrinology* **154** 3539–3551. (doi:10.1210/en.2012-2127)

Li L, Jick S, Gopalakrishnan C, Heide-Jorgensen U, Norrelund H, Sorensen HT, Christiansen CF & Ehrenstein V 2016 Metformin use and risk of lactic acidosis in people with diabetes with and without renal impairment: a cohort study in Denmark and the UK. *Diabetic Medicine* **34** 485–489. (doi:10.1111/dme.13203).

Litosch I 2016 Decoding Galphaq signaling. *Life Science* **152** 99–106. (doi:10.1016/j.lfs.2016.03.037)

Liu Y, Dentin R, Chen D, Hedrick S, Ravnskjaer K, Schenk S, Milne J, Meyers DJ, Cole P, Yates J 3rd, *et al*. 2008 A fasting inducible switch modulates gluconeogenesis via activator/coactivator exchange. *Nature* **456** 269–273. (doi:10.1038/nature07349)

Mathijs K, Kienhuis AS, Brauers KJ, Jennen DG, Lahoz A, Kleinjans JC & van Delft JH 2009 Assessing the metabolic competence of sandwich-cultured mouse primary hepatocytes. *Drug Metabolism and Disposition* **37** 1305–1311. (doi:10.1124/dmd.108.025775)

Mikoshiba K 2015 Role of IP3 receptor signaling in cell functions and diseases. *Advances in Biological Regulation* **57** 217–227. (doi:10.1016/j.jbior.2014.10.001)

Mitchell J 2013 Regulation of hepatic glucose production by Gq-coupled receptors: potential new targets for treatment of type 2 diabetes. *Endocrinology* **154** 3495–3497. (doi:10.1210/en.2013-1713)

Moller DE 2001 New drug targets for type 2 diabetes and the metabolic syndrome. *Nature* **414** 821–827. (doi:10.1038/414821a)

Nishimura A, Kitano K, Takasaki J, Taniguchi M, Mizuno N, Tago K, Hakoshima T & Itoh H 2010 Structural basis for the specific inhibition of heterotrimeric G(q) protein by a small molecule. *PNAS* **107** 13666–13671. (doi:10.1073/pnas.1003553107)

Omar A, Ellen R & Sorisky A 2016 Metformin-associated lactic acidosis in a patient with normal renal function. *Canadian Journal of Diabetes* **40** 280–281. (doi:10.1016/j.jcjd.2015.12.004)

Peng H, Want LL & Aroda VR 2016 Safety and tolerability of glucagon-like peptide-1 receptor agonists utilizing data from the exenatide clinical trial development program. *Current Diabetes Reports* **16** 44. (doi:10.1007/s11892-016-0728-4)

Perez-Garcia MJ, Cena V, de Pablo Y, Llovera M, Comella JX & Soler RM 2004 Glial cell line-derived neurotrophic factor increases intracellular calcium concentration. Role of calcium/calmodulin in the activation of the phosphatidylinositol 3-kinase pathway. *Journal of Biological Chemistry* **279** 6132–6142. (doi:10.1074/jbc.M308367200)

Pinto MC, Kihara AH, Goulart VA, Tonelli FM, Gomes KN, Ulrich H & Resende RR 2015 Calcium signaling and cell proliferation. *Cell Signaling* **27** 2139–2149. (doi:10.1016/j.cellsig.2015.08.006)

Puigserver P, Rhee J, Donovan J, Walkey CJ, Yoon JC, Oriente F, Kitamura Y, Altomonte J, Dong H, Accili D, *et al*. 2003 Insulin-regulated hepatic gluconeogenesis through FOXO1-PGC-1alpha interaction. *Nature* **423** 550–555. (doi:10.1038/nature01667)

Rah SY & Kim UH 2015 CD38-mediated Ca2+ signaling contributes to glucagon-induced hepatic gluconeogenesis. *Scientific Reports* **5** 10741. (doi:10.1038/srep10741)

Regard JB, Sato IT & Coughlin SR 2008 Anatomical profiling of G protein-coupled receptor expression. *Cell* **135** 561–571. (doi:10.1016/j.cell.2008.08.040)

Rena G, Pearson ER & Sakamoto K 2013 Molecular mechanism of action of metformin: old or new insights? *Diabetologia* **56** 1898–1906. (doi:10.1007/s00125-013-2991-0)

Rivera N, Everett-Grueter CA, Edgerton DS, Rodewald T, Neal DW, Nishimura E, Larsen MO, Jacobsen LO, Kristensen K, Brand CL, *et al*. 2007 A novel glucagon receptor antagonist, NNC 25-0926, blunts hepatic glucose production in the conscious dog. *Journal of Pharmacology and Experimental Therapeutics* **321** 743–752. (doi:10.1124/jpet.106.115717)

Rui L 2014 Energy metabolism in the liver. *Comprehensive Physiology* **4** 177–197. (doi:10.1002/cphy.c130024)

Saltiel AR & Kahn CR 2001 Insulin signalling and the regulation of glucose and lipid metabolism. *Nature* **414** 799–806. (doi:10.1038/414799a)

Sanchez-Fernandez G, Cabezudo S, Garcia-Hoz C, Beninca C, Aragay AM, Mayor F & Ribas C 2014 G alpha q signalling: the new and the old. *Cell Signaling* **26** 833–848. (doi:10.1016/j.cellsig.2014.01.010)

Scheen AJ 2016 Dulaglutide (LY-2189265) for the treatment of type 2 diabetes. *Expert Review of Clinical Pharmacology* **9** 385–399. (doi:10.1586/17512433.2016.1141046)

Schilling MM, Oeser JK, Boustead JN, Flemming BP & O'Brien RM 2006 Gluconeogenesis: re-evaluating the FOXO1-PGC-1alpha connection. *Nature* **443** E10–E11. (doi:10.1038/nature05288)

http://jme.endocrinology-journals.org
DOI: 10.1530/JME-17-0121

Published by Bioscientifica Ltd.

Shaw JE, Sicree RA & Zimmet PZ 2010 Global estimates of the prevalence of diabetes for 2010 and 2030. *Diabetes Research and Clinical Practice* **87** 4–14. (doi:10.1016/j.diabres.2009.10.007)

Siu FY, He M, de Graaf C, Han GW, Yang D, Zhang Z, Zhou C, Xu Q, Wacker D, Joseph JS, *et al*. 2013 Structure of the human glucagon class B G-protein-coupled receptor. *Nature* **499** 444–449. (doi:10.1038/nature12393)

Walker EH, Pacold ME, Perisic O, Stephens L, Hawkins PT, Wymann MP & Williams RL 2000 Structural determinants of phosphoinositide 3-kinase inhibition by wortmannin, LY294002, quercetin, myricetin, and staurosporine. *Molecular Cell* **6** 909–919. (doi:10.1016/S1097-2765(05)00089-4)

Wang Y, Inoue H, Ravnskjaer K, Viste K, Miller N, Liu Y, Hedrick S, Vera L & Montminy M 2010 Targeted disruption of the CREB coactivator Crtc2 increases insulin sensitivity. *PNAS* **107** 3087–3092. (doi:10.1073/pnas.0914897107)

Wang Y, Li G, Goode J, Paz JC, Ouyang K, Screaton R, Fischer WH, Chen J, Tabas I & Montminy M 2012 Inositol-1,4,5-trisphosphate receptor regulates hepatic gluconeogenesis in fasting and diabetes. *Nature* **485** 128–132. (doi:10.1038/nature10988)

Wang C, Chi Y, Li J, Miao Y, Li S, Su W, Jia S, Chen Z, Du S, Zhang X, *et al*. 2014 FAM3A activates PI3K p110alpha/Akt signaling to ameliorate hepatic gluconeogenesis and lipogenesis. *Hepatology* **59** 1779–1790. (doi:10.1002/hep.26945)

Xiong Y, Guo J, Candelore MR, Liang R, Miller C, Dallas-Yang Q, Jiang G, McCann PE, Qureshi SA, Tong X, *et al*. 2012 Discovery of a novel glucagon receptor antagonist N-[(4-{(1S)-1-[3-(3, 5-dichlorophenyl)-5-(6-methoxynaphthalen-2-yl)-1H-pyrazol-1-yl]ethyl}phenyl)carbo nyl]-beta-alanine (MK-0893) for the treatment of type II diabetes. *Journal of Medicinal Chemistry* **55** 6137–6148. (doi:10.1021/jm300579z)

Xu J, Zhang QG, Li C & Zhang GY 2007 Subtoxic N-methyl-D-aspartate delayed neuronal death in ischemic brain injury through TrkB receptor- and calmodulin-mediated PI-3K/Akt pathway activation. *Hippocampus* **17** 525–537. (doi:10.1002/hipo.20289)

Xu X, Wang G, Zhou T, Chen L, Chen J & Shen X 2014 Novel approaches to drug discovery for the treatment of type 2 diabetes. *Expert Opinion on Drug Discovery* **9** 1047–1058. (doi:10.1517/17460441.2014.941352)

Yang X, Mei S, Wang X, Li X, Liu R, Ma Y, Hao L, Yao P, Liu L, Sun X, *et al*. 2013 Leucine facilitates insulin signaling through a Galphai protein-dependent signaling pathway in hepatocytes. *Journal of Biological Chemistry* **288** 9313–9320. (doi:10.1074/jbc.M112.409409)

Yao XG, Xu X, Wang GH, Lei M, Quan LL, Cheng YH, Wan P, Zhou JP, Chen J, Hu LH, *et al*. 2015 BBT improves glucose homeostasis by ameliorating beta-cell dysfunction in type 2 diabetic mice. *Journal of Endocrinology* **224** 327–341. (doi:10.1530/JOE-14-0721)

Yoon JC, Puigserver P, Chen G, Donovan J, Wu Z, Rhee J, Adelmant G, Stafford J, Kahn CR, Granner DK, *et al*. 2001 Control of hepatic gluconeogenesis through the transcriptional coactivator PGC-1. *Nature* **413** 131–138. (doi:10.1038/35093050)

Zhang LN, Zhou HY, Fu YY, Li YY, Wu F, Gu M, Wu LY, Xia CM, Dong TC, Li JY, *et al*. 2013 Novel small-molecule PGC-1alpha transcriptional regulator with beneficial effects on diabetic db/db mice. *Diabetes* **62** 1297–1307. (doi:10.2337/db12-0703)

Zheng J, Woo SL, Hu X, Botchlett R, Chen L, Huo Y & Wu C 2015 Metformin and metabolic diseases: a focus on hepatic aspects. *Frontiers of Medicine* **9** 173–186. (doi:10.1007/s11684-015-0384-0)

Zhou TT, Quan LL, Chen LP, Du T, Sun KX, Zhang JC, Yu L, Li Y, Wan P, Chen LL, *et al*. 2016 SP6616 as a new Kv2.1 channel inhibitor efficiently promotes beta-cell survival involving both PKC/Erk1/2 and CaM/PI3K/Akt signaling pathways. *Cell Death and Disease* **7** e2216. (doi:10.1038/cddis.2016.119)

Zimmet P, Alberti KG & Shaw J 2001 Global and societal implications of the diabetes epidemic. *Nature* **414** 782–787. (doi:10.1038/414782a)

Received in final form 19 June 2017
Accepted 21 June 2017
Accepted Preprint published online 21 June 2017

http://jme.endocrinology-journals.org
DOI: 10.1530/JME-17-0121

Published by Bioscientifica Ltd.